Chapter 10

The General Circulation

In its broadest sense, the *general circulation* of the atmosphere is usually considered to include the totality of motions that characterizes the global-scale atmospheric flow. Specifically, the study of the general circulation is concerned with the dynamics of climate—that is, with the temporally averaged structures of the fields of wind, temperature, humidity, precipitation, and other meteorological variables. The general circulation may thus be considered to consist of the flow averaged in time over a period sufficiently long to remove the random variations associated with individual weather systems but short enough to retain monthly and seasonal variations.

In the past, both observational and theoretical studies of the general circulation concentrated on the dynamics of the zonally averaged flow. The time-averaged circulation is, however, highly dependent on longitude due to longitudinally asymmetric forcing by orography and land–sea heating contrasts. The longitudinally dependent components of the general circulation may be separated into *quasi-stationary circulations*, which vary little in time; *monsoonal circulations*, which are seasonally reversing; and various subseasonal and interannual components, which together account for *low-frequency variability*. A complete understanding of the physical basis for the general circulation requires an explanation not only for the zonally averaged circulation but for the longitudinally and time-varying components as well.

Nevertheless, to introduce the study of the general circulation, it proves useful to isolate those processes that maintain the zonal-mean flow (i.e., the flow averaged around latitude circles). This approach follows naturally from the linear wave studies of previous chapters in which flow fields were split into zonal-mean and longitudinally dependent eddy components. In this chapter, however, we concentrate not on the development and motion of the eddies but on the influence of the eddies on the structure of the zonal-mean circulation. Focusing on the zonal mean allows us to isolate those features of the circulation that are not dependent on continentality and should thus be common to all thermally driven rotating fluid systems. In particular, we discuss the angular momentum and energy budgets of the zonally averaged flow. We also show that the mean meridional circulation (i.e., the circulation consisting of the

An Introduction to Dynamic Meteorology. DOI: 10.1016/B978-0-12-384866-6.00010-6

zonal-mean vertical and meridional velocity components) satisfies a diagnostic equation analogous to the vertical motion equation of Section 6.5, but with the forcing determined by the distributions of diabatic heating and eddy heat and momentum fluxes.

Following our discussion of the zonal-mean circulation, we consider the longitudinally varying time-averaged circulation. In this chapter the primary emphasis is on extratropical aspects of the circulation; these can be discussed within the framework of quasi-geostrophic theory. The general circulation of the tropics is considered in Chapter 11.

10.1 THE NATURE OF THE PROBLEM

Theoretical speculation on the nature of the general circulation has quite a long history. Perhaps the most important early work on the subject was that of an 18th-century Englishman, George Hadley. Hadley, in seeking a cause for the trade wind circulation, realized that this circulation must be a form of thermal convection driven by the difference in solar heating between equatorial and polar regions. He visualized the general circulation as consisting of a zonally symmetric overturning in which the heated equatorial air rises and flows poleward, where it cools, sinks, and flows equatorward again. At the same time, the Coriolis force deflects the poleward moving air at the upper levels to the east and the equatorward-moving air near the surface to the west. The latter is, of course, consistent with the observed surface winds in the trade wind zone, which are northeasterly in the Northern Hemisphere and southeasterly in the Southern Hemisphere. This type of circulation is now called a *Hadley circulation* or *Hadley cell*.

Although a circulation consisting of Hadley cells extending from equator to pole in each hemisphere is mathematically possible in the sense that such a circulation would not violate the laws of physics, the observed Hadley circulation is confined to the tropics. Evidence from a number of studies indicates that for conditions existing in Earth's atmosphere, a symmetric hemispheric-wide Hadley circulation would be baroclinically unstable. If such a circulation were to become established by some mechanism, it would quickly break down outside the tropics as baroclinic eddies developed and modified the zonal-mean circulation through their heat and momentum fluxes.

The observed general circulation thus cannot be understood purely in terms of zonally symmetric processes. Rather, it can be thought of qualitatively as developing through three-dimensional interactions among radiative and dynamical processes. In the mean, the net solar energy absorbed by the atmosphere and Earth must equal the infrared energy radiated back to space by the planet. The annually averaged solar heating is, however, strongly dependent on latitude, with a maximum at the equator and a minimum at the poles. The outgoing infrared radiation, however, is only weakly latitude dependent. Thus, there is a net radiation surplus in the equatorial region and a deficit in the polar region.

This differential heating warms the equatorial atmosphere relative to higher latitudes and creates a pole-to-equator temperature gradient. Therefore, it produces a growing store of zonal-mean available potential energy. At some point the westerly thermal wind (which must develop if the motion is to be balanced geostrophically in the presence of the pole-to-equator temperature gradient) becomes baroclinically unstable. As shown in Chapter 8, the resulting baroclinic waves transport heat poleward. These waves will intensify until their heat transport (together with the heat transported by planetary waves and ocean currents) is sufficient to balance the radiation deficit in the polar regions so that the pole-to-equator temperature gradient ceases to grow. At the same time, these perturbations convert potential energy into kinetic energy, thereby maintaining the kinetic energy of the atmosphere against the effects of frictional dissipation.

From a thermodynamic point of view, the atmosphere may be regarded as a "heat engine" that absorbs net heat at relatively warm temperatures in the tropics (primarily in the form of latent heat due to evaporation from the sea surface) and gives up heat at relatively cool temperatures in the extratropics. In this manner, net radiation generates available potential energy, which is in turn partially converted to kinetic energy, which does work to maintain the circulation against frictional dissipation. Only a small fraction of the solar energy input is actually converted to kinetic energy. Thus, from an engineer's viewpoint, the atmosphere is a rather inefficient heat engine. However, if due account is taken of the many constraints operating on atmospheric motions, it appears that the atmosphere may in fact generate kinetic energy about as efficiently as dynamically possible.

The preceding qualitative discussion suggests that the gross features of the general circulation outside the tropics can be understood on the basis of quasi-geostrophic theory, since, as we have seen, baroclinic instability is contained within the quasi-geostrophic framework. In view of this fact, and to keep the equations as simple as possible, our discussion of the zonally averaged and longitudinally varying components of the circulation outside the tropics will concentrate on those aspects that can be qualitatively represented by the quasi-geostrophic equations on the midlatitude β plane.

It should be recognized that a quasi-geostrophic model cannot provide a complete theory of the general circulation because in the quasi-geostrophic theory a number of assumptions are made concerning scales of motion that restrict in advance the possible types of solutions. Quantitative modeling of the general circulation requires complicated numerical models based on the primitive equations in spherical coordinates. The ultimate objective of these modeling efforts is to simulate the general circulation so faithfully that the climatological consequences of any change in the external parameters (e.g., the atmospheric concentration of carbon dioxide) can be predicted accurately. Present models can provide fairly accurate simulations of the current climate and plausible predictions of the response of the climate system to changes in external conditions.

However, uncertainties in the representations of a number of physical processes, particularly clouds and precipitation, limit the confidence that can be placed in quantitative climate change predictions based on such models.

10.2 THE ZONALLY AVERAGED CIRCULATION

The observed global distribution of the longitudinally averaged zonal wind for the two solstice seasons was shown in Figure 6.1. Although there are important interhemispheric differences, the flow in both hemispheres is characterized by westerly jets with maximum zonal velocities at about 30° to 35° latitude near the tropopause. These westerlies vary in longitude, especially in the Northern Hemisphere (refer to Figure 6.2), but there is a significant zonally symmetric component, which we will refer to as the *mean zonal wind*.

Although departures of the time-averaged flow from zonal symmetry are important aspects of the general circulation, especially in the Northern Hemisphere, it is useful to first obtain an understanding of the dynamics of the zonally symmetric component before investigating the three-dimensional time-mean circulation. This section examines the dynamics of zonally symmetric motions using quasi-geostrophic theory and the log-pressure coordinate system introduced in Chapter 7, and shows that the meridional circulation associated with an axially symmetric vortex is dynamically analogous to the secondary divergent circulation in a baroclinic wave.

In the log-pressure coordinate system, the x and y components of the momentum equation, the hydrostatic approximation, the continuity equation, and the thermodynamic energy equation can be written as

$$Du/Dt - fv + \partial\Phi/\partial x = X \tag{10.1}$$

$$Dv/Dt + fu + \partial\Phi/\partial y = Y \tag{10.2}$$

$$\partial\Phi/\partial z = H^{-1}RT \tag{10.3}$$

$$\partial u/\partial x + \partial v/\partial y + \rho_0^{-1}\partial\left(\rho_0 w\right)/\partial z = 0 \tag{10.4}$$

$$DT/Dt + (\kappa T/H)\, w = J/c_p \tag{10.5}$$

where

$$\frac{D}{Dt} \equiv \frac{\partial}{\partial t} + u\frac{\partial}{\partial x} + v\frac{\partial}{\partial y} + w\frac{\partial}{\partial z}$$

and X and Y designate the zonal and meridional components of drag due to small-scale eddies.

For convenience in this and the following chapters, we have dropped the asterisk notation used in Chapter 7 to distinguish the log-pressure coordinate from geometric height. Thus, z here designates the log-pressure variable defined in Section 7.4.1.

Analysis of the zonally averaged circulation involves study of the interaction of longitudinally varying disturbances (referred to as eddies and denoted by primed variables) with the longitudinally averaged flow (referred to as the mean flow and denoted by overbars). Thus, any variable A is expanded in the form $A = \overline{A} + A'$. This sort of average is a *Eulerian mean*, as it is evaluated at fixed latitude, height, and time. Eulerian mean equations are obtained by taking zonal averages of (10.1) through (10.5). Such averaging is facilitated by using (10.4) to expand the material derivative for any variable A in flux form as follows:

$$\begin{aligned}\rho_0 \frac{DA}{Dt} &= \rho_0 \left(\frac{\partial}{\partial t} + \mathbf{V} \cdot \nabla + w \frac{\partial}{\partial z} \right) A + A \left[\nabla \cdot (\rho_0 \mathbf{V}) + \frac{\partial}{\partial z} (\rho_0 w) \right] \\ &= \frac{\partial}{\partial t} (\rho_0 A) + \frac{\partial}{\partial x} (\rho_0 A u) + \frac{\partial}{\partial y} (\rho_0 A v) + \frac{\partial}{\partial z} (\rho_0 A w)\end{aligned} \tag{10.6}$$

where we recall that $\rho_0 = \rho_0(z)$.

Applying the zonal averaging operator then gives

$$\rho_0 \overline{\frac{DA}{Dt}} = \frac{\partial}{\partial t} \left(\rho_0 \overline{A} \right) + \frac{\partial}{\partial y} \left[\rho_0 \left(\overline{A} \overline{v} + \overline{A' v'} \right) \right] + \frac{\partial}{\partial z} \left[\rho_0 \left(\overline{A} \overline{w} + \overline{A' w'} \right) \right] \tag{10.7}$$

Here we have used the fact that $\partial \overline{(\,)}/\partial x = 0$, since quantities with the overbar are independent of x. We have also used the fact that for any variables a and b

$$\overline{ab} = \overline{(\overline{a} + a')\left(\overline{b} + b'\right)} = \overline{\overline{a}\overline{b}} + \overline{\overline{a}b'} + \overline{a'\overline{b}} + \overline{a'b'} = \overline{a}\overline{b} + \overline{a'b'}$$

which follows from that fact that $\overline{a}$ and $\overline{b}$ are independent of x and $\overline{a'} = \overline{b'} = 0$ so that, for example, $\overline{\overline{a}b'} = \overline{a}\overline{b'} = 0$.

The terms involving $(\overline{v}, \overline{w})$ on the right in (10.7) can be rewritten in advective form with the aid of the zonal mean of (10.4):

$$\partial \overline{v}/\partial y + \rho_0^{-1} \partial (\rho_0 \overline{w})/\partial z = 0 \tag{10.8}$$

Applying the chain rule of differentiation to the mean terms on the right in (10.7) and substituting from (10.8), we can rewrite (10.7) as

$$\rho_0 \overline{\frac{DA}{Dt}} = \rho_0 \frac{\overline{D}}{Dt} \left(\overline{A} \right) + \frac{\partial}{\partial y} \left[\rho_0 \left(\overline{A' v'} \right) \right] + \frac{\partial}{\partial z} \left[\rho_0 \left(\overline{A' w'} \right) \right] \tag{10.9}$$

where

$$\frac{\overline{D}}{Dt} \equiv \frac{\partial}{\partial t} + \overline{v}\frac{\partial}{\partial y} + \overline{w}\frac{\partial}{\partial z} \tag{10.10}$$

is the rate of change following the mean meridional motion $(\overline{v}, \overline{w})$.

10.2.1 The Conventional Eulerian Mean

Applying the averaging scheme of (10.9) to (10.1) and (10.5), we obtain the zonal-mean zonal momentum and thermodynamic energy equations for quasi-geostrophic motions on the midlatitude β plane:

$$\partial\overline{u}/\partial t - f_0\overline{v} = -\partial\left(\overline{u'v'}\right)/\partial y + \overline{X} \tag{10.11}$$

$$\partial\overline{T}/\partial t + N^2 H R^{-1}\overline{w} = -\partial\left(\overline{v'T'}\right)/\partial y + \overline{J}/c_p \tag{10.12}$$

where N is the buoyancy frequency defined by

$$N^2 \equiv \frac{R}{H}\left(\frac{\kappa T_0}{H} + \frac{dT_0}{dz}\right)$$

In (10.11) and (10.12), consistent with quasi-geostrophic scaling, we have neglected advection by the ageostrophic mean meridional circulation and vertical eddy flux divergences. It is easily confirmed that for quasi-geostrophic scales, these terms are small compared to the retained terms (see Problem 10.4). We have included the zonally averaged turbulent drag in (10.11) because stresses due to unresolved eddies (such as gravity waves) may be important not only in the boundary layer but also in the upper troposphere and in the middle atmosphere.

Similar scaling shows that the zonal average of the meridional momentum equation (10.2) can be approximated accurately by geostrophic balance:

$$f_0\overline{u} = -\partial\overline{\Phi}/\partial y$$

This can be combined with the hydrostatic approximation (10.3) to give the thermal wind relation

$$f_0\partial\overline{u}/\partial z + RH^{-1}\partial\overline{T}/\partial y = 0 \tag{10.13}$$

This relationship between zonal-mean wind and potential temperature distributions imposes a strong constraint on the ageostrophic mean meridional circulation $(\overline{v}, \overline{w})$. In the absence of a mean meridional circulation, the eddy momentum flux divergence in (10.11) and eddy heat flux divergence in (10.12) would tend separately to change the mean zonal wind and temperature fields, and thus would destroy thermal wind balance. The pressure gradient force that

results from any small departure of the mean zonal wind from geostrophic balance will, however, drive a mean meridional circulation, which adjusts the mean zonal wind and temperature fields so that (10.13) remains valid. In many situations this compensation allows the mean zonal wind to remain unchanged even in the presence of large eddy heat and momentum fluxes. The mean meridional circulation thus plays exactly the same role in the zonal-mean circulation that the secondary divergent circulation plays in the synoptic-scale quasi-geostrophic system. In fact, for steady-state mean flow conditions, the $(\overline{v}, \overline{w})$ circulation must just balance the eddy forcing plus diabatic heating so that the balances in (10.11) and (10.12) are as follows:

- Coriolis force $(f_0\overline{v}) \approx$ divergence of eddy momentum fluxes
- Adiabatic cooling $\approx$ diabatic heating plus convergence of eddy heat fluxes

Analysis of observations shows that outside the tropics these balances appear to be approximately true above the boundary layer. Thus, changes in the zonal-mean flow arise from small imbalances between the forcing terms and the mean meridional circulation.

The Eulerian mean meridional circulation can be determined in terms of the forcing from an equation similar to the omega equation of Section 6.4. Before deriving this equation, it is useful to observe that the mean meridional mass circulation is nondivergent in the meridional plane. Thus, it can be represented in terms of a meridional mass transport streamfunction, which identically satisfies the continuity equation (10.8) by letting

$$\rho_0\overline{v} = -\frac{\partial\overline{\chi}}{\partial z}; \quad \rho_0\overline{w} = \frac{\partial\overline{\chi}}{\partial y} \tag{10.14}$$

The relationship of the sign of the streamfunction $\overline{\chi}$ to the sense of the mean meridional circulation is shown schematically in Figure 10.1.

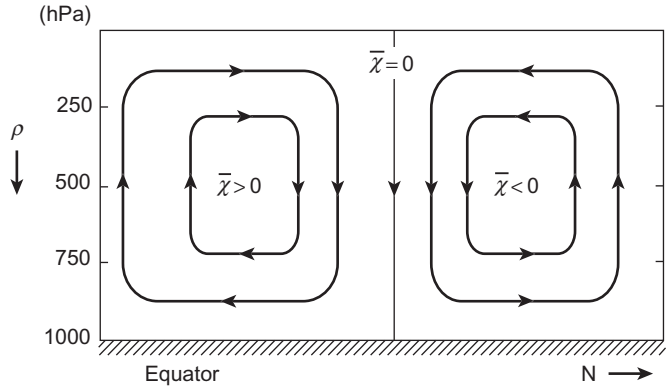

FIGURE 10.1 Relationship of the Eulerian mean meridional streamfunction to vertical and meridional motion.

The diagnostic equation for $\overline{\chi}$ is derived by first taking

$$f_0 \frac{\partial}{\partial z}(10.11) + \frac{R}{H}\frac{\partial}{\partial y}(10.12)$$

and then using (10.13) to eliminate the time derivatives and (10.14) to express the mean meridional circulation in terms of $\overline{\chi}$. The resulting elliptic equation has the form

$$\frac{\partial^2 \overline{\chi}}{\partial y^2} + \frac{f_0^2}{N^2}\rho_0 \frac{\partial}{\partial z}\left(\frac{1}{\rho_0}\frac{\partial \overline{\chi}}{\partial z}\right) = \frac{\rho_0}{N^2}\left[\frac{\partial}{\partial y}\left(\frac{\kappa \overline{J}}{H} - \frac{R}{H}\frac{\partial}{\partial y}\left(\overline{v'T'}\right)\right) - f_0\left(\frac{\partial^2}{\partial z \partial y}\left(\overline{u'v'}\right) - \frac{\partial \overline{X}}{\partial z}\right)\right] \tag{10.15}$$

Equation (10.15) can be used to qualitatively diagnose the mean meridional circulation. Because $\overline{\chi}$ must vanish on the boundaries, it can be represented by a double Fourier series in y and z. Hence, the elliptic operator on the left side of (10.15) is approximately proportional to $-\overline{\chi}$, and (10.15) states qualitatively that

$$\overline{\chi} \propto -\frac{\partial}{\partial y}(\text{diabatic heating}) + \frac{\partial^2}{\partial y^2}(\text{large-scale eddy heat flux}) + \frac{\partial^2}{\partial y \partial z}(\text{large-scale eddy momentum flux}) + \frac{\partial}{\partial z}(\text{zonal drag force})$$

Now, diabatic heating in the Northern Hemisphere decreases for increasing y. Thus, the first term on the right is positive and tends to force a mean meridional cell with $\overline{\chi} > 0$. This is referred to as a *thermally direct* cell, as warm air is rising and cool air is sinking. It is this process that primarily accounts for the Hadley circulation of the tropics as illustrated in Figure 10.2. For an idealized Hadley cell in the absence of eddy sources, the differential diabatic heating would be balanced only by adiabatic cooling near the equator and adiabatic warming at higher latitudes.

In the extratropical Northern Hemisphere, poleward eddy heat fluxes due to both transient synoptic-scale eddies and stationary planetary waves tend to transfer heat poleward, producing a maximum poleward heat flux $\overline{v'T'}$ in the lower troposphere at about 50° latitude as shown in Figure 10.3. Because $\overline{\chi}$ is proportional to the second derivative of $\overline{v'T'}$, which should be negative where $\overline{v'T'} > 0$, the term should tend to produce a mean meridional cell with $\overline{\chi} < 0$ centered in the lower troposphere at midlatitudes. Thus, the eddy heat flux tends to drive an indirect meridional circulation.

The existence of this indirect meridional circulation can be understood in terms of the need to maintain geostrophic and hydrostatic balance. North of the latitude where $\overline{v'T'}$ is a maximum, there is a convergence of eddy heat flux,

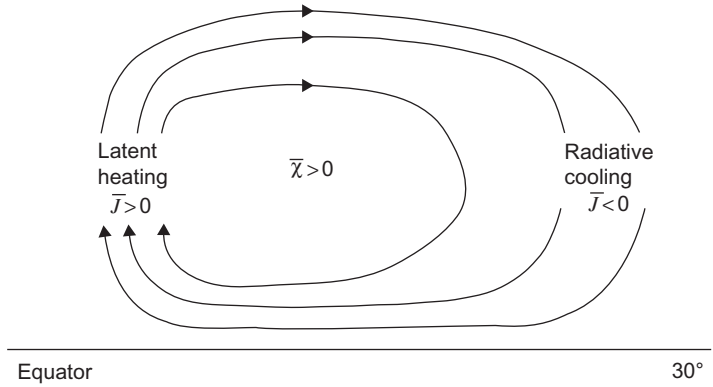

FIGURE 10.2 Schematic Eulerian mean meridional circulation showing the streamfunction for a thermally direct Hadley cell.

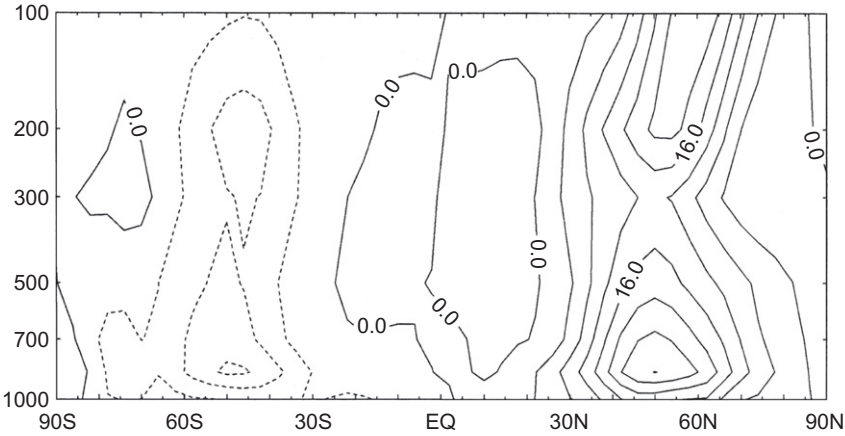

FIGURE 10.3 Observed northward eddy heat flux distribution ($^{\circ}\mathrm{C\,m\,s^{-1}}$) for Northern Hemisphere winter. (*Adapted from Schubert et al., 1990.*)

while equatorward of that latitude, there is a divergence. Thus, eddy heat transport tends to reduce the pole-to-equator mean temperature gradient. If the mean zonal flow is to remain geostrophic, the thermal wind must then also decrease. In the absence of eddy momentum transport, this decrease in the thermal wind can only be produced by the Coriolis torque due to a mean meridional circulation with the sense of that in Figure 10.4. At the same time, it is not surprising to find that the vertical mean motions required by continuity oppose the temperature tendency associated with the eddy heat flux by producing adiabatic warming in the region of eddy heat flux divergence and adiabatic cooling in the region of eddy heat flux convergence.

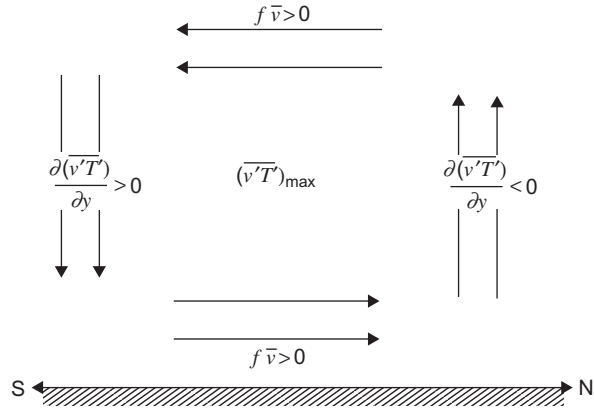

FIGURE 10.4 Schematic Eulerian mean meridional circulation forced by poleward heat fluxes.

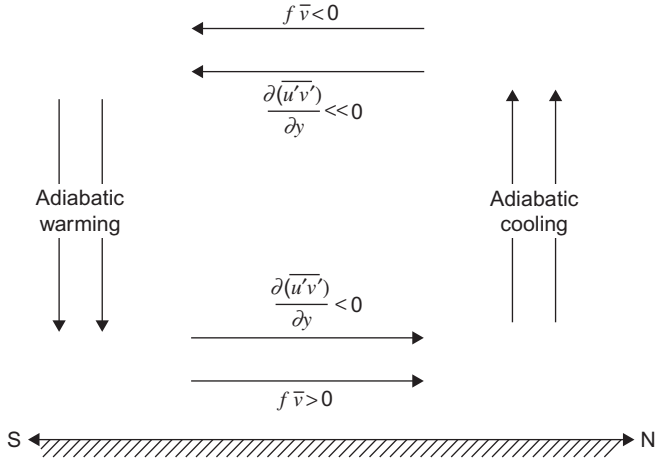

FIGURE 10.5 Schematic Eulerian mean meridional circulation forced by a vertical gradient in eddy momentum flux convergence.

The next to last forcing term in (10.15) is proportional to the vertical gradient of the horizontal eddy momentum flux convergence. However, it can be shown (see Problem 10.5) that

$$-\frac{\partial^2}{\partial z \partial y}\left(\overline{u'v'}\right) = +\frac{\partial}{\partial z}\left(\overline{v'\zeta'}\right)$$

Thus, this term is proportional to the vertical derivative of the meridional vorticity flux. To interpret this eddy forcing physically, we suppose as shown in Figure 10.5 that the momentum flux convergence (or the vorticity flux) is positive and increasing with height. This will be true in the Northern Hemisphere

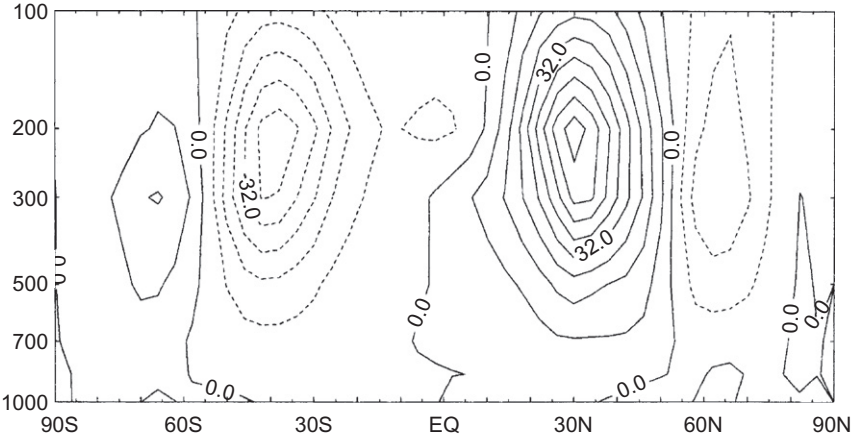

FIGURE 10.6 Observed northward eddy momentum flux distribution ($m^2\ s^{-2}$) for Northern Hemisphere winter. (*Adapted from Schubert et al., 1990.*)

troposphere poleward of the core of the jet stream, as $\overline{u'v'}$ tends to be poleward and to reach its maximum near the tropopause at about 30° (at the core of the mean jetstream) as shown in Figure 10.6. For this configuration of momentum flux, $\partial^2\overline{u'v'}/\partial y\partial z < 0$ in the midlatitude troposphere, which again drives a mean meridional cell with $\overline{\chi} < 0$. From (10.11) it is clear that the Coriolis force of this induced indirect meridional circulation is required to balance the acceleration due to the momentum flux convergence, which would otherwise increase the vertical shear of the mean zonal wind and destroy the thermal wind balance.

Thus, the combined eddy heat flux and the eddy momentum flux distributions tend to drive mean meridional cells in each hemisphere with rising motion poleward of 45° and sinking motion equatorward of 45°. This eddy forcing more than compensates the direct diabatic drive at midlatitudes and is responsible for the observed thermally indirect *Ferrel cell*.

The resultant observed climatology of the Eulerian mean meridional circulation is shown in Figure 10.7. It consists primarily of tropical Hadley cells driven by diabatic heating and eddy-driven midlatitude Ferrel cells. There are also minor thermally direct cells at polar latitudes. The meridional circulation in the winter is much stronger than that in the summer, especially in the Northern Hemisphere. This reflects the seasonal variation both in the diabatic and in the eddy flux forcing terms in (10.15).

The Ferrel cell presents a conundrum, since the vertical circulations produced by individual baroclinic eddies are thermally direct, with warm air rising and cold air sinking. Yet, the Eulerian mean meridional circulation, which averages over these circulations, shows a thermally indirect circulation. This conundrum is resolved by examining the meridional circulation in isentropic

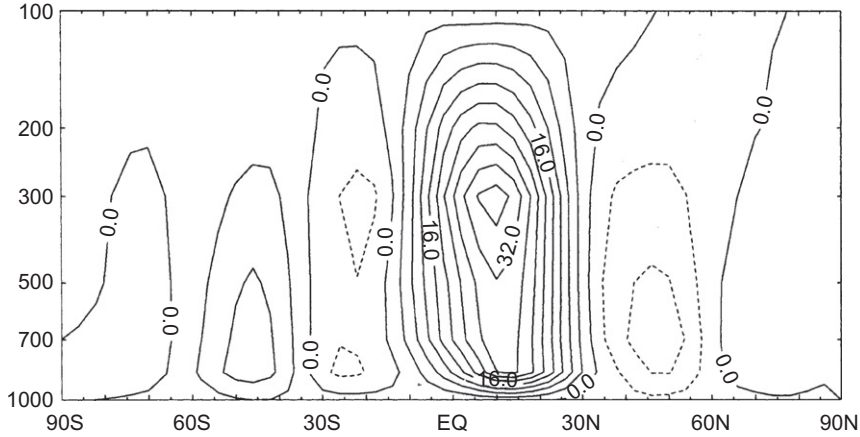

FIGURE 10.7 Streamfunction (units: 10^2 kg m^{-1}s^{-1}) for the observed Eulerian mean meridional circulation for Northern Hemisphere winter. (*Based on the data of Schubert et al., 1990*).

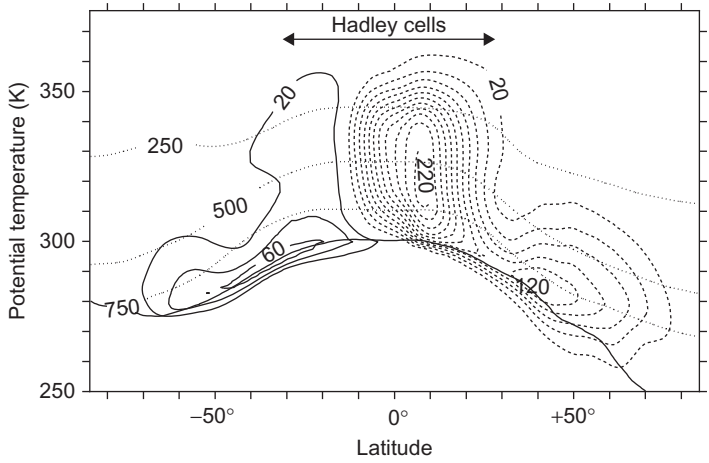

FIGURE 10.8 January time and zonal-mean isentropic mass flux streamfunction determined from ERA-40 reanalysis data 1980–2001). *Streamfunction contours* are shown every 20×10^9 kg s^{-1}, with implied clockwise circulation around negative values. *Dotted lines* show pressure surfaces and the *solid lower curve* is the median surface potential temperature. (*Adapted from Schneider, 2006. Used with permission of Annual Reviews.*)

coordinates (Figure 10.8), which reveals a thermally direct circulation in both the Hadley cells and in the extratropics. This shows that the Ferrel cell is an artifact of the Eulerian averaging process and that eddy fluxes of entropy are large compared to those of the mean circulation.

The zonal momentum balance in the upper troposphere in tropical and mid-latitude cells is maintained by the balance between the Coriolis force caused

by the mean meridional drift and the eddy momentum flux convergence. The heat balance is maintained by rising motion (adiabatic cooling) balancing the diabatic heating in the tropics and by the eddy heat flux convergence at high latitudes and subsidence (adiabatic warming) balancing the eddy heat flux divergence in the subtropics.

Because of the appearance of eddy flux terms in both mean momentum and thermodynamic energy equations, and the near cancellation of eddy and mean flow processes, it is rather inefficient to attempt to diagnose the net eddy forcing of the mean flow from the conventional Eulerian mean. It can be shown that similar eddy and mean flow compensation occurs in the Eulerian mean continuity equation for a long-lived tracer so that tracer transport calculations are also inefficient in this formulation.

10.2.2 The Transformed Eulerian Mean

An alternative approach to analysis of the zonal-mean circulation, which provides a clearer diagnosis of eddy forcing and also provides a more direct view of transport processes in the meridional plane, is the *transformed Eulerian mean* (TEM) formulation introduced by Andrews and McIntyre (1976). This transformation takes account of the fact that in (10.12) there tends to be a strong cancellation between the eddy heat flux convergence and adiabatic cooling, while the diabatic heating term is a small residual. Since in the mean an air parcel will rise to a higher equilibrium altitude only if its potential temperature is increased by diabatic heating, it is the *residual meridional circulation* associated with diabatic processes that is directly related to the mean meridional mass flow.

The TEM equations can be obtained from (10.11) and (10.12) by defining the residual circulation $\left(\overline{v}^*, \overline{w}^*\right)$ as follows:

$$\overline{v}^* = \overline{v} - \rho_0^{-1} RH^{-1} \partial(\rho_0 \overline{v'T'}/N^2)/\partial z \tag{10.16a}$$

$$\overline{w}^* = \overline{w} + RH^{-1} \partial(\overline{v'T'}/N^2)/\partial y \tag{10.16b}$$

The residual vertical velocity defined in this manner clearly represents that part of the mean vertical velocity with a contribution to adiabatic temperature change that is not canceled by the eddy heat flux divergence.

Substituting from (10.16a) into (10.11) and (10.12) to eliminate $(\overline{v}, \overline{w})$ yields the TEM equations

$$\partial \overline{u}/\partial t - f_0 \overline{v}^* = +\rho_0^{-1} \nabla \cdot \mathbf{F} + \overline{X} \equiv \overline{G} \tag{10.17}$$

$$\partial \overline{T}/\partial t + N^2 H R^{-1} \overline{w}^* = \overline{J}/c_p \tag{10.18}$$

$$\partial \overline{v}^*/\partial y + \rho_0^{-1} \partial \left(\rho_0 \overline{w}^*\right)/\partial z = 0 \tag{10.19}$$

where $\mathbf{F} \equiv \mathbf{j}F_y + \mathbf{k}F_z$, the *Eliassen–Palm flux* (EP flux), is a vector in the meridional (y, z) plane, which for large-scale quasi-geostrophic eddies has the components

$$F_y = -\rho_0 \overline{u'v'}, \quad F_z = \rho_0 f_0 R \overline{v'T'} \big/ (N^2 H) \tag{10.20}$$

and $\overline{G}$ in (10.17) designates the total zonal force due to both large- and small-scale eddies.

The TEM formulation clearly shows that the eddy heat and momentum fluxes do not act separately to drive changes in the zonal-mean circulation, but only in the combination given by the divergence of the EP flux. The fundamental role of the eddies is thus to exert a zonal force. This eddy forcing of the zonal-mean flow can be displayed conveniently by mapping the field of $\mathbf{F}$ and contouring the isolines of its divergence. When properly scaled by the basic state density, these contours give the zonal force per unit mass exerted by quasi-geostrophic eddies. The mean global EP flux divergence pattern for a Northern Hemisphere winter is shown in Figure 10.9. Note that in most of the extratropical troposphere, the EP flux is convergent so that the eddies exert a westward zonal force on the atmosphere. On the seasonal time scale the zonal force due to the EP flux divergence in (10.17) is nearly balanced by the eastward Coriolis force of the residual mean meridional circulation. Conditions for this balance are discussed in the next subsection.

The structure of the residual mean meridional circulation can be determined by defining a residual streamfunction:

$$\overline{\chi}^* \equiv \overline{\chi} + \rho_0 \frac{R}{H} \frac{\overline{v'T'}}{N^2}$$

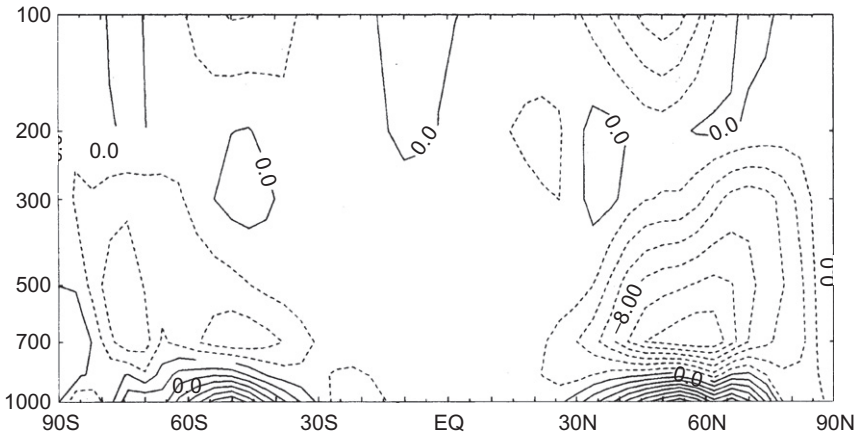

FIGURE 10.9 Eliassen–Palm flux divergence divided by the standard density ρ_0 for Northern Hemisphere winter. (Units: m s^{-1} day^{-1}.) (*Based on the data of Schubert et al., 1990.*)

It can then be shown by direct substitution into (10.14) and (10.15) that

$$\rho_0 \overline{v}^* = -\frac{\partial \overline{\chi}^*}{\partial z}; \quad \rho_0 \overline{w}^* = \frac{\partial \overline{\chi}^*}{\partial y}$$

and

$$\frac{\partial^2 \overline{\chi}^*}{\partial y^2} + \rho_0 \frac{f_0^2}{N^2} \frac{\partial}{\partial z}\left(\frac{1}{\rho_0}\frac{\partial \overline{\chi}^*}{\partial z}\right) = \frac{\rho_0}{N^2}\left[\frac{\partial}{\partial y}\left(\frac{\kappa \overline{J}}{H}\right) + f_0 \frac{\partial \overline{G}}{\partial z}\right] \tag{10.21}$$

The magnitudes of the diabatic and EP flux contributions to the source term on the right in (10.21) are generally larger in the winter hemisphere than in the summer hemisphere. In the Northern Hemisphere troposphere, the source terms are generally negative, whereas in the Southern Hemisphere, they are generally positive. This implies that $\overline{\chi}^*$ itself is positive in the Northern Hemisphere and negative in the Southern Hemisphere so that the residual meridional circulation consists of a single thermally direct overturning in each hemisphere, with the strongest cell in the winter hemisphere as shown in Figure 10.10.

Unlike the conventional Eulerian mean, the residual mean vertical motion for time-averaged conditions is proportional to the rate of diabatic heating. It approximately represents the *diabatic circulation* in the meridional plane—that is, the circulation in which parcels that rise are diabatically heated and those that sink are diabatically cooled in order that their potential temperatures adjust to the local environment. The time-averaged residual mean meridional circulation thus approximates the mean motion of air parcels and thus, unlike the conventional Eulerian mean, provides an approximation to the mean advective transport of trace substances.

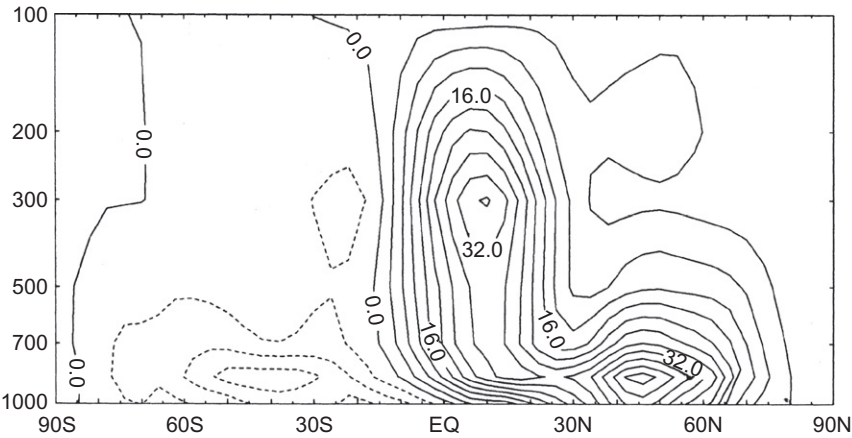

FIGURE 10.10 Residual mean meridional streamfunction (units: 10^2 kg m^{-1} s^{-1}) for Northern Hemisphere winter. (*Based on the data of Schubert et al., 1990.*)

10.2.3 The Zonal-Mean Potential Vorticity Equation

Further insight into the nature of the extratropical zonal-mean circulation can be obtained by zonally averaging the quasi-geostrophic potential vorticity equation to obtain

$$\partial \overline{q} \,/ \partial t = -\partial \left(\overline{q'v'} \right) / \partial y \tag{10.22}$$

where the zonal-mean potential vorticity is

$$\overline{q} = f_0 + \beta y + \frac{1}{f_0} \frac{\partial^2 \overline{\Phi}}{\partial y^2} + \frac{f_0}{\rho_0} \frac{\partial}{\partial z} \left(\frac{\rho_0}{N^2} \frac{\partial \overline{\Phi}}{\partial z} \right) \tag{10.23}$$

and the eddy potential vorticity is

$$q' = \frac{1}{f_0} \left(\frac{\partial^2 \Phi'}{\partial x^2} + \frac{\partial^2 \Phi'}{\partial y^2} \right) + \frac{f_0}{\rho_0} \frac{\partial}{\partial z} \left(\frac{\rho_0}{N^2} \frac{\partial \Phi'}{\partial z} \right) \tag{10.24}$$

The quantity $\overline{q'v'}$ on the right in (10.22) is the divergence of the meridional flux of potential vorticity. According to (10.22), for adiabatic quasi-geostrophic flow, the mean distribution of potential vorticity can be changed only if there is a nonzero flux of eddy potential vorticity. The zonal-mean potential vorticity, together with suitable boundary conditions on $\overline{\Phi}$, completely determines the distribution of zonal-mean geopotential and thus the zonal-mean geostrophic wind and temperature distributions. Thus, eddy-driven mean flow accelerations require nonzero potential vorticity fluxes.

It can be shown that the potential vorticity flux is related to the eddy momentum and heat fluxes. We first note that for quasi-geostrophic motions, the eddy horizontal velocities in the flux terms are geostrophic:

$$f_0 v' = \partial \Phi' \,/ \partial x \quad \text{and} \quad f_0 u' = -\partial \Phi' \,/ \partial y$$

Thus,

$$\overline{v' \frac{\partial^2 \Phi'}{\partial x^2}} = \frac{1}{f_0} \overline{\frac{\partial \Phi'}{\partial x} \frac{\partial^2 \Phi'}{\partial x^2}} = \frac{1}{2f_0} \overline{\frac{\partial}{\partial x} \left(\frac{\partial \Phi'}{\partial x} \right)^2} = 0$$

where we have used the fact that a perfect differential in x vanishes when averaged zonally. Thus,

$$\overline{q'v'} = \overline{\frac{v'}{f_0} \frac{\partial^2 \Phi'}{\partial y^2}} + \frac{f_0}{\rho_0} \overline{v' \frac{\partial}{\partial z} \left(\frac{\rho_0}{N^2} \frac{\partial \Phi'}{\partial z} \right)}$$

We can use the chain rule of differentiation to rewrite the terms on the right in this expression as

$$\overline{\frac{v'}{f_0}\frac{\partial^2\Phi'}{\partial y^2}} = \frac{1}{f_0^2}\left(\overline{\frac{\partial\Phi'}{\partial x}\frac{\partial^2\Phi'}{\partial y^2}}\right)$$

$$= \frac{1}{f_0^2}\left[\frac{\partial}{\partial y}\left(\overline{\frac{\partial\Phi'}{\partial x}\frac{\partial\Phi'}{\partial y}}\right) - \frac{1}{2}\frac{\partial}{\partial x}\overline{\left(\frac{\partial\Phi'}{\partial y}\right)^2}\right] = -\frac{\partial}{\partial y}\left(\overline{u'v'}\right)$$

and

$$\frac{f_0}{\rho_0}\overline{v'\frac{\partial}{\partial z}\left(\frac{\rho_0}{N^2}\frac{\partial\Phi'}{\partial z}\right)} = \frac{1}{\rho_0}\left[\frac{\partial}{\partial z}\left(\frac{\rho_0}{N^2}\overline{\frac{\partial\Phi'}{\partial x}\frac{\partial\Phi'}{\partial z}}\right) - \frac{\rho_0}{2N^2}\frac{\partial}{\partial x}\overline{\left(\frac{\partial\Phi'}{\partial z}\right)^2}\right]$$

$$= \frac{f_0}{\rho_0}\frac{\partial}{\partial z}\left(\frac{\rho_0}{N^2}\overline{v'\frac{\partial\Phi'}{\partial z}}\right)$$

Thus,

$$\overline{q'v'} = -\frac{\partial\overline{u'v'}}{\partial y} + \frac{f_0}{\rho_0}\frac{\partial}{\partial z}\left(\frac{\rho_0}{N^2}\overline{v'\frac{\partial\Phi'}{\partial z}}\right) \tag{10.25}$$

so that it is not the momentum flux $\overline{u'v'}$ or heat flux $\overline{v'\partial\Phi'/\partial z}$ that drives net changes in the mean flow distribution, but rather the combination given by the potential vorticity flux. Under some circumstances the eddy momentum flux and eddy heat flux may individually be large, but the combination in (10.25) actually vanishes. This cancellation effect makes the traditional Eulerian mean formulation a poor framework for analysis of mean flow forcing by eddies.

Comparing (10.25) and (10.20), we see that the potential vorticity flux is proportional to the divergence of the EP flux vector:

$$\overline{q'v'} = \rho_0^{-1}\nabla\cdot\mathbf{F} \tag{10.26}$$

Thus, the contribution of large-scale motions to the zonal force in (10.17) equals the meridional flux of quasi-geostrophic potential vorticity. If the motion is adiabatic and the potential vorticity flux is nonzero, equation (10.22) shows that the mean flow distribution must change with time. For this reason, there cannot be complete compensation between Coriolis torque and zonal force terms in (10.17).

10.3 THE ANGULAR MOMENTUM BUDGET

The previous section used the quasi-geostrophic version of the zonal-mean equations to show that large-scale eddies play an essential part in the maintenance of the zonal-mean circulation in the extratropics. In particular, we

contrasted the mean flow forcing as represented by the conventional Eulerian mean and TEM formulations. This section expands our consideration of the momentum budget by considering the overall balance of *angular* momentum for the atmosphere and Earth combined. Thus, rather than simply considering the balance of momentum for a given latitude and height in the atmosphere, we must consider the transfer of angular momentum between Earth and the atmosphere, and the flow of angular momentum in the atmosphere.

It would be possible to utilize the complete spherical coordinate version of the TEM equations for this analysis, but we are concerned primarily with the angular momentum balance for a zonal ring of air extending from the surface to the top of the atmosphere. In that case it proves simpler to use the conventional Eulerian mean formulation. It also proves convenient to use a special vertical coordinate, called the *sigma coordinate*, in which Earth's surface is a coordinate surface.

Because the average rotation rate of Earth is itself observed to be very close to constant, the atmosphere must also on the average conserve its angular momentum. The atmosphere gains angular momentum from Earth in the tropics where the surface winds are easterly (i.e., where the angular momentum of the atmosphere is less than that of Earth) and gives up angular momentum to Earth in middle latitudes where the surface winds are westerly. Thus, there must be a net poleward transport of angular momentum within the atmosphere; otherwise, the torque due to surface friction would decelerate both easterlies and westerlies. Furthermore, the angular momentum given by Earth to the atmosphere in the belt of easterlies must just balance the angular momentum given up to Earth in the westerlies if the global angular momentum of the atmosphere is to remain constant.

In the equatorial regions the poleward angular momentum transport is divided between the advection of absolute angular momentum by the poleward flow in the axially symmetric Hadley circulation and transport by eddies. In midlatitudes, however, it is primarily the eddy motions that transport momentum poleward, and the angular momentum budget of the atmosphere must be qualitatively as shown in Figure 10.11.

As this figure suggests, there is a maximum poleward flux of angular momentum at about 30° latitude and a maximum horizontal flux convergence at about 45°. This maximum in the flux convergence is a reflection of the strong energy conversion in upper-level westerlies and is the mechanism whereby the atmosphere can maintain a positive zonal wind in the middle latitudes despite the momentum lost to the surface.

It is convenient to analyze the momentum budget in terms of absolute angular momentum. The absolute angular momentum per unit mass of atmosphere is

$$M = (\Omega a \cos\phi + u)\, a \cos\phi$$

where as before a is the radius of Earth. The crucial role of zonal eddy drag in maintaining the observed latitudinal profile of the mean zonal wind can be

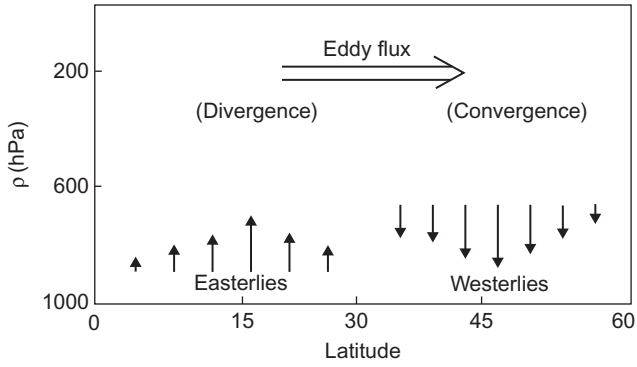

FIGURE 10.11 Schematic mean angular momentum budget for the atmosphere–Earth system.

seen by evaluating the mean zonal velocity that would arise if a zonal ring of air at rest on the equator were to be displaced poleward, conserving M. In that case $u(\phi) = \Omega a \sin^2 \phi / \cos \phi$, so that in an angular momentum–conserving Hadley circulation, $u \approx 130\,\mathrm{m\,s^{-1}}$ at 30° latitude, which is far greater than is observed.

Clearly, the absolute angular momentum must decrease as air parcels are advected poleward in the Hadley circulation. The absolute angular momentum of an individual air parcel can be changed only by torques caused by the zonal pressure gradient and eddy stresses. In isobaric coordinates, Newton's second law in its angular momentum form is thus

$$\frac{DM}{Dt} = -a \cos \phi \left[\frac{\partial \Phi}{\partial x} + g \frac{\partial \tau_E^x}{\partial p} \right] \tag{10.27}$$

where τ_E^x is the zonal component of the vertical eddy stress, and it is assumed that horizontal eddy stresses are negligible compared to the vertical eddy stress.

10.3.1 Sigma Coordinates

In neither the isobaric nor the log-pressure coordinate system does the lower boundary exactly coincide with a coordinate surface. In analytical studies it is usual to assume that the lower boundary can be approximated as a constant pressure surface and to apply the approximate condition

$$\omega(p_s) \approx -\rho_0 g w(z_0)$$

as the lower boundary condition. Here we have assumed that the height of the ground z_0 is coincident with the pressure surface p_s–that is, where p_s is usually set equal to 1000 hPa. These assumptions are of course not strictly valid even when the ground is level. Pressure does change at the ground, but, more

important, the height of the ground generally varies so that even if the pressure tendency were zero everywhere, the lower boundary condition should not be applied at a constant p_s. Rather, we should set $p_s = p_s(x, y)$. It is very inconvenient for mathematical analysis, however, to have a boundary condition that must be applied at a surface that is a function of the horizontal variables.

This problem can be overcome by defining a vertical coordinate that is proportional to pressure normalized by the surface pressure. The most common form of this coordinate is the *sigma coordinate,* defined as $\sigma \equiv p/p_s$, where $p_s(x, y, t)$ is the pressure at the surface. Thus, σ is a nondimensional-independent vertical coordinate that decreases upward from a value of $\sigma = 1$ at the ground to $\sigma = 0$ at the top of the atmosphere. In sigma coordinates the lower boundary condition will always apply exactly at $\sigma = 1$. Furthermore, the vertical σ velocity defined by

$$\dot{\sigma} \equiv D\sigma/Dt$$

will always be zero at the ground even in the presence of sloping terrain. Thus, the lower boundary condition in the σ system is merely

$$\dot{\sigma} = 0 \text{ at } \sigma = 1$$

To transform the dynamical equations from the isobaric system to the σ system, we first transform the pressure gradient force in a manner analogous to that shown in Section 1.4.3. Applying (1.36) with p replaced by Φ, s replaced by σ, and z replaced by p, we find that

$$(\partial\Phi/\partial x)_\sigma = (\partial\Phi/\partial x)_p + \sigma(\partial \ln p_s/\partial x)(\partial\Phi/\partial\sigma) \tag{10.28}$$

Because any other variable will transform in an analogous way, we can write the general transformation as

$$\nabla_p(\ ) = \nabla_\sigma(\ ) - \sigma\nabla \ln p_s \partial(\ )/\partial\sigma \tag{10.29}$$

Applying the transformation (10.29) to the momentum equation (3.2), we get

$$\frac{D\mathbf{V}}{Dt} + f\mathbf{k} \times \mathbf{V} = -\nabla\Phi + \sigma\nabla \ln p_s \frac{\partial\Phi}{\partial\sigma} \tag{10.30}$$

where ∇ is now applied holding σ constant, and the total differential is

$$\frac{D}{Dt} = \frac{\partial}{\partial t} + \mathbf{V} \cdot \nabla + \dot{\sigma}\frac{\partial}{\partial\sigma} \tag{10.31}$$

The equation of continuity can be transformed to the σ system by first using (10.29) to express the divergence of the horizontal wind as

$$\nabla_p \cdot \mathbf{V} = \nabla_\sigma \cdot \mathbf{V} - \sigma(\nabla \ln p_s) \cdot \partial\mathbf{V}/\partial\sigma \tag{10.32}$$

To transform the term $\partial\omega/\partial p$, we first note that since p_s does not depend on σ

$$\frac{\partial}{\partial p} = \frac{\partial}{\partial(\sigma p_s)} = \frac{1}{p_s}\frac{\partial}{\partial\sigma}$$

Thus, the continuity equation (3.5) can be written as

$$p_s\left(\nabla_p \cdot \mathbf{V}\right) + \partial\omega/\partial\sigma = 0 \tag{10.33}$$

Now the sigma vertical velocity can be written as

$$\dot{\sigma} = \left(\frac{\partial\sigma}{\partial t} + \mathbf{V}\cdot\nabla\sigma\right)_p + \omega\frac{\partial\sigma}{\partial p} = -\frac{\sigma}{p_s}\left(\frac{\partial p_s}{\partial t} + \mathbf{V}\cdot\nabla p_s\right) + \frac{\omega}{p_s}$$

Differentiating the preceding with respect to σ, eliminating $\partial\omega/\partial\sigma$ with (10.33), and rearranging yields the transformed continuity equation

$$\frac{\partial p_s}{\partial t} + \nabla\cdot\left(p_s\mathbf{V}\right) + p_s\frac{\partial\dot{\sigma}}{\partial\sigma} = 0 \tag{10.34}$$

With the aid of the equation of state and Poisson's equation–that is, (2.44)—the hydrostatic approximation can be written in the sigma system as

$$\frac{\partial\Phi}{\partial\sigma} = -\frac{RT}{\sigma} = -\frac{R\theta}{\sigma}\left(p/p_0\right)^{\kappa} \tag{10.35}$$

where $p_0 = 1000\,\text{hPa}$.

Expanding the total derivative in (2.46), we may write the thermodynamic energy equation for sigma coordinates as

$$\frac{\partial\theta}{\partial t} + \mathbf{V}\cdot\nabla\theta + \dot{\sigma}\frac{\partial\theta}{\partial\sigma} = \frac{J}{c_p}\frac{\theta}{T} \tag{10.36}$$

10.3.2 The Zonal-Mean Angular Momentum

We now transform the angular momentum equation (10.27) into sigma coordinates with the aid of (10.28) and (10.35) to yield

$$\left(\frac{\partial}{\partial t} + \mathbf{V}\cdot\nabla + \dot{\sigma}\frac{\partial}{\partial\sigma}\right)M = -a\cos\phi\left(\frac{\partial\Phi}{\partial x} + \frac{RT}{p_s}\frac{\partial p_s}{\partial x} + \frac{g}{p_s}\frac{\partial\tau_E^x}{\partial\sigma}\right) \tag{10.37}$$

Multiplying the continuity equation (10.34) by M and adding the result to (10.37) multiplied by p_s, we obtain the flux form of the angular momentum

equation[1]:

$$\frac{\partial (p_s M)}{\partial t} = -\nabla \cdot (p_s M \mathbf{V}) - \frac{\partial (p_s M \dot{\sigma})}{\partial \sigma} - a\cos\phi \left[p_s \frac{\partial \Phi}{\partial x} + RT \frac{\partial p_s}{\partial x} \right] - ga\cos\phi \frac{\partial \tau_E^x}{\partial \sigma} \tag{10.38}$$

To obtain the zonal-mean angular momentum budget, we must average (10.38) in longitude. Using the spherical coordinate expansion for the horizontal divergence as given in Appendix C, we have

$$\nabla \cdot (p_s M \mathbf{V}) = \frac{1}{a\cos\phi} \left[\frac{\partial (p_s M u)}{\partial \lambda} + \frac{\partial (p_s M v \cos\phi)}{\partial \phi} \right] \tag{10.39}$$

We also observe that the bracketed term on the right in equation (10.38) can be rewritten as

$$\left[p_s \frac{\partial}{\partial x} (\Phi - RT) + \frac{\partial}{\partial x} (p_s RT) \right] \tag{10.40}$$

However, with the aid of the hydrostatic equation (10.35), we can write

$$(\Phi - RT) = \Phi + \sigma \partial \Phi \big/ \partial \sigma = \partial (\sigma \Phi) \big/ \partial \sigma$$

Thus, recalling that p_s does not depend on σ, we obtain

$$\left[p_s \frac{\partial \Phi}{\partial x} + RT \frac{\partial p_s}{\partial x} \right] = \left[\frac{\partial}{\partial \sigma} \left(p_s \sigma \frac{\partial \Phi}{\partial x} \right) + \frac{\partial}{\partial x} (p_s RT) \right] \tag{10.41}$$

Substituting from (10.39) and (10.41) into (10.38) and taking the zonal average gives

$$\frac{\partial \overline{(p_s M)}}{\partial t} = -\frac{1}{\cos\phi} \frac{\partial}{\partial y} \left(\overline{p_s M v} \cos\phi \right) - \frac{\partial}{\partial \sigma} \left[\overline{p_s M \dot{\sigma}} + ga\cos\phi \left(\overline{\tau}_E^x \right) + (a\cos\phi) \sigma \overline{p_s \frac{\partial \Phi}{\partial x}} \right] \tag{10.42}$$

The terms on the right in (10.42) represent the convergence of the horizontal flux of angular momentum and the convergence of the vertical flux of angular momentum, respectively.

[1] It may be shown (Problem 10.2) that in sigma coordinates, the mass element $\rho_0 dxdydz$ takes the form $-g^{-1} p_s dxdyd\sigma$. Thus, p_s in sigma space plays a role similar to density in physical space.

Integrating (10.42) vertically from Earth's surface ($\sigma = 1$) to the top of the atmosphere ($\sigma = 0$), and recalling that $\dot{\sigma} = 0$ for $\sigma = 0, 1$, we have

$$\int_0^1 g^{-1} \frac{\partial}{\partial t} \overline{p_s M} d\sigma = -(g \cos\phi)^{-1} \int_0^1 \frac{\partial}{\partial y} \left(\overline{p_s M v} \cos\phi\right) d\sigma - a \cos\phi \left[\left(\overline{\tau_E^x}\right)_{\sigma=1} + \overline{p_s \partial h / \partial x}\right] \tag{10.43}$$

where $h(x, y) = g^{-1}\Phi(x, y, 1)$ is the height of the lower boundary ($\sigma = 1$), and we have assumed that the eddy stress vanishes at $\sigma = 0$.

Equation (10.43) expresses the angular momentum budget for a zonal ring of air of unit meridional width, extending from the ground to the top of the atmosphere. In the long-term mean the three terms on the right, representing the convergence of the meridional flux of angular momentum, the torque due to small-scale turbulent fluxes at the surface, and the surface pressure torque, must balance. In the sigma coordinate system the surface pressure torque takes the particularly simple form $-\overline{p_s \partial h / \partial x}$. Thus, the pressure torque acts to transfer angular momentum from the atmosphere to the ground, provided that the surface pressure and the slope of the ground ($\partial h / \partial x$) are correlated positively. Observations indicate that this is generally the case in middle latitudes because there is a slight tendency for the surface pressure to be higher on the western sides of mountains than on the eastern sides (refer to Figure 4.11). In midlatitudes of the Northern Hemisphere the surface pressure torque provides nearly one-half of the total atmosphere–surface momentum exchange, but in the tropics and the Southern Hemisphere the exchange is dominated by turbulent eddy stresses.

The role of eddy motions in providing the meridional angular momentum transport necessary to balance the surface angular momentum sinks can be elucidated best if we divide the flow into zonal-mean and eddy components by letting

$$M = \overline{M} + M' = \left(\Omega a \cos\phi + \overline{u} + u'\right) a \cos\phi$$

$$p_s v = \overline{(p_s v)} + (p_s v)'$$

where primes indicate deviations from the zonal-mean. Thus, the meridional flux becomes

$$\overline{(p_s M v)} = \left[\Omega a \cos\phi \overline{p_s v} + \overline{u} \overline{p_s v} + \overline{u' (p_s v)'}\right] a \cos\phi \tag{10.44}$$

The three meridional flux terms on the right in this expression are called the meridional Ω–momentum flux, the meridional drift, and the meridional eddy momentum flux, respectively.

The drift term is important in the tropics, but in midlatitudes it is small compared to the eddy flux and can be neglected in an approximate treatment. Furthermore, we can show that the meridional Ω–momentum flux does not contribute to the vertically integrated flux. Averaging the continuity equation (10.34) zonally and integrating vertically, we obtain

$$\overline{\frac{\partial p_s}{\partial t}} = -(\cos\phi)^{-1}\frac{\partial}{\partial y}\int_0^1 \overline{p_s v}\cos\phi d\sigma \tag{10.45}$$

Thus, for time-averaged flow—where the left side of (10.45) vanishes—there is no net mass flow across latitude circles. The vertically integrated meridional angular momentum flux is therefore given approximately by

$$\int_0^1 \overline{p_s M v}d\sigma \approx \int_0^1 \overline{u'(p_s v)'}a\cos\phi d\sigma \approx \int_0^1 a\cos\phi\overline{p}_s\overline{u'v'}d\sigma \tag{10.46}$$

where we have assumed that the fractional change in p_s is small compared to the change in v' so that $(p_s v)' \approx \overline{p}_s v'$. The angular momentum flux is thus proportional to the negative of the meridional component of the EP flux given in (10.20).

In the Northern Hemisphere, as shown in Figure 10.6, the eddy momentum flux in midlatitudes is positive and decreases in magnitude with latitude poleward of 30°. For quasi-geostrophic flow, positive eddy momentum flux requires that the eddies be asymmetric in the horizontal plane, with the trough and ridge axes tilting as indicated in Figure 10.12. When the troughs and ridges on the average have southwest to northeast phase tilt, the zonal flow will be larger than average ($u' > 0$) where the meridional flow is poleward ($v' > 0$) and less than average ($u' < 0$) where the flow is equatorward. Thus, $\overline{u'v'} > 0$, and the eddies will systematically transport positive zonal momentum poleward.

As shown in (10.42), the total vertical momentum flux consists of the flux due to large-scale motions $\overline{p_s M\dot{\sigma}} \approx \Omega a\cos\phi\overline{p_s\dot{\sigma}}$; the flux due to the pressure

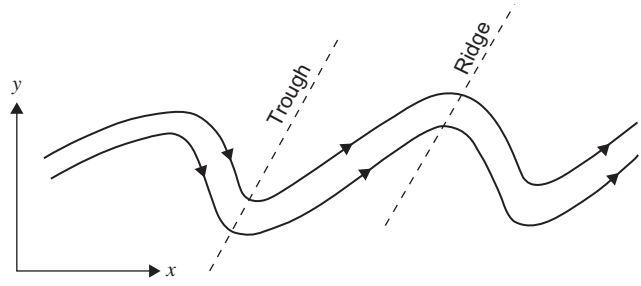

FIGURE 10.12 Schematic streamlines for a positive eddy momentum flux.

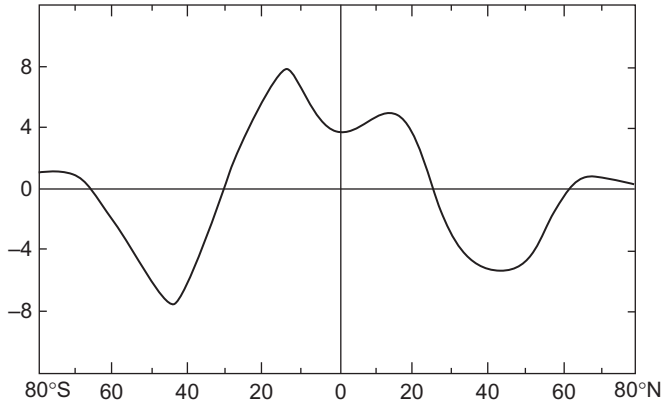

FIGURE 10.13 Latitudinal profile of the annual mean eastward torque (surface friction plus mountain torque) exerted on the atmosphere in units of 10^{18} m^2 kg s^{-2}. (*Adapted from Oort and Peixoto, 1983.*)

torque, $(a\cos\phi)\overline{\sigma p_s \partial\Phi / \partial x}$; and the flux due to small-scale turbulent stresses, $ga\cos\phi\overline{\tau_E^x}$. As mentioned previously, the last two are responsible for the transfer of momentum from Earth to the atmosphere in the tropics and from the atmosphere to Earth in midlatitudes. Outside the planetary boundary layer, however, the vertical momentum transport in the troposphere is due primarily to the vertical Ω–momentum flux, $\Omega a\cos\phi\overline{p_s\dot{\sigma}}$.

An estimate of the annual average of the zonal-mean total surface torque is shown in Figure 10.13. The total surface torque must be balanced by poleward fluxes of angular momentum in the atmosphere. Except for the belt within 10° of the equator, almost all of the poleward flux is accounted for by the eddy flux term given on the right side of (10.46). Thus, the momentum budget and the energy cycle both depend critically on the transports by the eddies.

10.4 THE LORENZ ENERGY CYCLE

The previous section discussed the interaction between zonally averaged flow and longitudinally varying eddy motions in terms of the angular momentum balance. It is also useful to examine the exchange of energy between the eddies and the mean flow. As in Section 10.2, we limit the analysis to quasi-geostrophic flow on a midlatitude β plane. Eulerian mean equations in log-pressure coordinates can then be written as

$$\partial\overline{u}/\partial t - f_0\overline{v} = -\partial\left(\overline{u'v'}\right)/\partial y + \overline{X} \tag{10.47}$$

$$f_0\overline{u} = -\partial\overline{\Phi}/\partial y \tag{10.48}$$

$$\frac{\partial}{\partial t}\left(\frac{\partial \overline{\Phi}}{\partial z}\right) + \overline{w}N^2 = \frac{\kappa}{H}\overline{J} - \frac{\partial}{\partial y}\left(\overline{v'\frac{\partial \Phi'}{\partial z}}\right) \tag{10.49}$$

$$\partial \overline{v}/\partial y + \rho_0^{-1}\partial(\rho_0 \overline{w})/\partial z = 0 \tag{10.50}$$

Here we have used the hydrostatic approximation in (10.3) to express the temperature in (10.49) in terms of the differential geopotential thickness, and we have again neglected vertical eddy fluxes and advection by the mean meridional circulation in (10.47) and (10.49). We have, however, included a turbulent drag force, $\overline{X}$, in (10.47), as dissipation by unresolved turbulent eddies is an essential element in the energy balance.

To analyze the exchange of energy between mean flow and eddies, we require a similar set of dynamical equations for the eddy motion. For simplicity, assume that the eddies satisfy the following linearized set of equations[2]:

$$\left(\frac{\partial}{\partial t} + \overline{u}\frac{\partial}{\partial x}\right)u' - \left(f_0 - \frac{\partial \overline{u}}{\partial y}\right)v' = -\frac{\partial \Phi'}{\partial x} + X' \tag{10.51}$$

$$\left(\frac{\partial}{\partial t} + \overline{u}\frac{\partial}{\partial x}\right)v' + f_0 u' = -\frac{\partial \Phi'}{\partial y} + Y' \tag{10.52}$$

$$\left(\frac{\partial}{\partial t} + \overline{u}\frac{\partial}{\partial x}\right)\frac{\partial \Phi'}{\partial z} + v'\frac{\partial}{\partial y}\left(\frac{\partial \overline{\Phi}}{\partial z}\right) + N^2 w' = \frac{\kappa J'}{H} \tag{10.53}$$

$$\frac{\partial u'}{\partial x} + \frac{\partial v'}{\partial y} + \frac{1}{\rho_0}\frac{\partial\left(\rho_0 w'\right)}{\partial z} = 0 \tag{10.54}$$

where X' and Y' are the zonally varying components of drag as a result of unresolved turbulent motions.

We now define a global average:

$$\langle\ \rangle \equiv A^{-1}\int_0^{\infty}\int_0^{D}\int_0^{L}(\ )dxdydz$$

where L is the distance around a latitude circle, D is the meridional extent of the midlatitude β plane, and A designates the total horizontal area of the β plane.

[2]A similar analysis can be carried out for the nonlinear case.

Then for any quantity Ψ

$$\begin{aligned}
\langle \partial\Psi/\partial x\rangle &= 0 \\
\langle \partial\Psi/\partial y\rangle &= 0, \quad \text{if } \Psi \text{ vanishes at } y = \pm D \\
\langle \partial\Psi/\partial z\rangle &= 0, \quad \text{if } \Psi \text{ vanishes at } z = 0 \text{ and } z \to \infty
\end{aligned}$$

An equation for the evolution of the mean flow kinetic energy can then be obtained by multiplying (10.47) by $\rho_0\overline{u}$ and (10.48) by $\rho_0\overline{v}$ and adding the results to get

$$\begin{aligned}
\rho_0\frac{\partial}{\partial t}\left(\frac{\overline{u}^2}{2}\right) &= -\rho_0\overline{v}\frac{\partial\overline{\Phi}}{\partial y} - \rho_0\overline{u}\frac{\partial}{\partial y}\left(\overline{u'v'}\right) + \rho_0\overline{u}\overline{X} \\
&= -\frac{\partial}{\partial y}\left(\rho_0\overline{v}\overline{\Phi}\right) + \rho_0\overline{\Phi}\frac{\partial\overline{v}}{\partial y} - \frac{\partial}{\partial y}\left(\rho_0\overline{u}\overline{u'v'}\right) + \rho_0\overline{u'v'}\frac{\partial\overline{u}}{\partial y} + \rho_0\overline{u}\overline{X}
\end{aligned}$$

Integrating over the entire volume, we get

$$\frac{d}{dt}\left\langle\frac{\rho_0\overline{u}^2}{2}\right\rangle = +\left\langle\rho_0\overline{\Phi}\frac{\partial\overline{v}}{\partial y}\right\rangle + \left\langle\rho_0\overline{u'v'}\frac{\partial\overline{u}}{\partial y}\right\rangle + \left\langle\rho_0\overline{u}\overline{X}\right\rangle \tag{10.55}$$

where we have assumed that $\overline{v} = 0$ and $\overline{u'v'} = 0$ for $y = \pm D$. Terms on the right side in (10.55) can be interpreted as the work done by the zonal-mean pressure force, the conversion of eddy kinetic energy to zonal-mean kinetic energy, and dissipation by the zonal-mean eddy stress. Alternatively, the first term on the right can be rewritten with the aid of the continuity equation to yield

$$\left\langle\rho_0\overline{\Phi}\frac{\partial\overline{v}}{\partial y}\right\rangle = -\left\langle\overline{\Phi}\frac{\partial\rho_0\overline{w}}{\partial z}\right\rangle = \left\langle\rho_0\overline{w}\frac{\partial\overline{\Phi}}{\partial z}\right\rangle = \frac{R}{H}\left\langle\rho_0\overline{w}\overline{T}\right\rangle$$

where we have assumed that $\rho_0\overline{w} = 0$ at $z = 0$, and $z \to \infty$. Thus, averaged over the whole domain the pressure work term is proportional to the correlation between the zonal-mean vertical mass flux $\rho_0\overline{w}$ and the zonal-mean temperature (or thickness). This term will be positive if on the average warm air is rising and cold air is sinking—that is, if there is a conversion from potential to kinetic energy.

Section 7.3.1 showed that in the quasi-geostrophic system the available potential energy is proportional to the square of the deviation of temperature from a standard atmosphere profile divided by the static stability. In terms of differential thickness the zonal-mean available potential energy is defined as

$$\overline{P} \equiv \frac{1}{2}\left\langle\frac{\rho_0}{N^2}\left(\frac{\partial\overline{\Phi}}{\partial z}\right)^2\right\rangle$$

Multiplying (10.49) through by $\rho_0(\partial\overline{\Phi}/\partial z)/N^2$ and averaging over space gives

$$\frac{d}{dt}\left\langle \frac{\rho_0}{2N^2}\left(\frac{\partial\overline{\Phi}}{\partial z}\right)^2\right\rangle = -\left\langle \rho_0\overline{w}\frac{\partial\overline{\Phi}}{\partial z}\right\rangle + \left\langle \frac{\rho_0\kappa\bar{J}}{N^2H}\left(\frac{\partial\overline{\Phi}}{\partial z}\right)\right\rangle - \left\langle \frac{\rho_0}{N^2}\frac{\partial\overline{\Phi}}{\partial z}\frac{\partial}{\partial y}\left(\overline{v'\frac{\partial\Phi'}{\partial z}}\right)\right\rangle \tag{10.56}$$

The first term on the right is just equal and opposite to the first term on the right in (10.55), which confirms that this term represents a conversion between zonal-mean kinetic and potential energies. The second term involves the correlation between temperature and diabatic heating; it expresses the generation of zonal-mean potential energy by diabatic processes. The final term, which involves the meridional eddy heat flux, expresses the conversion between zonal-mean and eddy potential energy.

That the second term on the right in (10.55) and the final term in (10.56) represent conversion between zonal-mean and eddy energies can be confirmed by performing analogous operations on the eddy equations (10.51), (10.52), and (10.53) to obtain equations for the eddy kinetic and available potential energies:

$$\frac{d}{dt}\left\langle \rho_0\frac{\overline{u'^2}+\overline{v'^2}}{2}\right\rangle = +\left\langle \rho_0\overline{\Phi'\left(\frac{\partial u'}{\partial x}+\frac{\partial v'}{\partial y}\right)}\right\rangle - \left\langle \rho_0\overline{u'v'}\frac{\partial\overline{u}}{\partial y}\right\rangle + \left\langle \rho_0\left(\overline{u'X'}+\overline{v'Y'}\right)\right\rangle \tag{10.57}$$

$$\frac{d}{dt}\left\langle \frac{\rho_0}{2N^2}\overline{\left(\frac{\partial\Phi'}{\partial z}\right)^2}\right\rangle = -\left\langle \rho_0\overline{w'\frac{\partial\Phi'}{\partial z}}\right\rangle + \left\langle \frac{\rho_0\kappa\overline{J'\partial\Phi'/\partial z}}{N^2H}\right\rangle - \left\langle \frac{\rho_0}{N^2}\left(\frac{\partial^2\overline{\Phi}}{\partial z\partial y}\right)\left(\overline{v'\frac{\partial\Phi'}{\partial z}}\right)\right\rangle \tag{10.58}$$

If we set $w' = 0$ at $z = 0$, the first term on the right in (10.57) can be rewritten using the continuity equation (10.54) as

$$\left\langle \rho_0\overline{\Phi'\left(\frac{\partial u'}{\partial x}+\frac{\partial v'}{\partial y}\right)}\right\rangle = -\left\langle \overline{\Phi'\frac{\partial(\rho_0 w')}{\partial z}}\right\rangle = \left\langle \rho_0\overline{w'\left(\frac{\partial\Phi'}{\partial z}\right)}\right\rangle$$

which is equal to minus the first term on the right in (10.58). Thus, this term expresses the conversion between eddy kinetic and eddy potential energy for the Eulerian mean formulation. Similarly, the last term in (10.58) is equal to

minus the last term in (10.56) and thus represents conversion between eddy and zonal-mean available potential energy.

The Lorenz energy cycle can be expressed compactly by defining zonal-mean and eddy kinetic and available potential energies:

$$\overline{K} \equiv \left\langle \rho_0 \frac{\overline{u}^2}{2} \right\rangle, \quad K' \equiv \left\langle \rho_0 \frac{\overline{u'^2} + \overline{v'^2}}{2} \right\rangle$$

$$\overline{P} \equiv \frac{1}{2} \left\langle \frac{\rho_0}{N^2} \left(\frac{\partial \overline{\Phi}}{\partial z} \right)^2 \right\rangle, \quad P' \equiv \frac{1}{2} \left\langle \frac{\rho_0}{N^2} \overline{\left(\frac{\partial \Phi'}{\partial z} \right)^2} \right\rangle$$

the energy transformations

$$\left[\overline{P} \cdot \overline{K}\right] \equiv \left\langle \rho_0 \overline{w} \frac{\partial \overline{\Phi}}{\partial z} \right\rangle, \quad \left[P' \cdot K'\right] \equiv \left\langle \rho_0 \overline{w' \frac{\partial \Phi'}{\partial z}} \right\rangle$$

$$\left[K' \cdot \overline{K}\right] \equiv \left\langle \rho_0 \overline{u'v'} \frac{\partial \overline{u}}{\partial y} \right\rangle, \quad \left[P' \cdot \overline{P}\right] \equiv \left\langle \frac{\rho_0}{N^2} \overline{v' \frac{\partial \Phi'}{\partial z}} \frac{\partial^2 \overline{\Phi}}{\partial y \partial z} \right\rangle$$

and the sources and sinks

$$\overline{R} \equiv \left\langle \frac{\rho_0}{N^2} \frac{\kappa \overline{J}}{H} \frac{\partial \overline{\Phi}}{\partial z} \right\rangle, \quad R' \equiv \left\langle \frac{\rho_0}{N^2} \overline{\frac{\kappa J'}{H} \frac{\partial \Phi'}{\partial z}} \right\rangle$$

$$\overline{\varepsilon} \equiv \left\langle \rho_0 \overline{u} \overline{X} \right\rangle, \quad \varepsilon' \equiv \left\langle \rho_0 \left(\overline{u'X'} + \overline{v'Y'} \right) \right\rangle$$

Equations (10.55) through (10.58) can then be expressed in the simple form

$$d\overline{K}/dt = \left[\overline{P} \cdot \overline{K}\right] + \left[K' \cdot \overline{K}\right] + \overline{\varepsilon} \tag{10.59}$$

$$d\overline{P}/dt = -\left[\overline{P} \cdot \overline{K}\right] + \left[P' \cdot \overline{P}\right] + \overline{R} \tag{10.60}$$

$$dK'/dt = \left[P' \cdot K'\right] - \left[K' \cdot \overline{K}\right] + \varepsilon' \tag{10.61}$$

$$dP'/dt = -\left[P' \cdot K'\right] - \left[P' \cdot \overline{P}\right] + R' \tag{10.62}$$

Here $[A \cdot B]$ designates conversion from energy form A to form B.

Adding (10.59) through (10.62), we obtain an equation for the rate of change of total energy (kinetic plus available potential):

$$d\left(\overline{K} + K' + \overline{P} + P'\right)/dt = \overline{R} + R' + \overline{\varepsilon} + \varepsilon' \tag{10.63}$$

For adiabatic inviscid flow, the right side vanishes and the total energy $\overline{K} + K' + \overline{P} + P'$ is conserved. In this system the zonal-mean kinetic energy does not include a contribution from the mean meridional flow because the zonally averaged meridional momentum equation was replaced by the geostrophic

approximation. (Likewise, use of the hydrostatic approximation means that neither the mean nor the eddy vertical motion is included in the total kinetic energy.) Thus, the quantities that are included in the total energy depend on the particular model used. For any model the definitions of energy must be consistent with the approximations employed.

In the long-term mean, the left side of (10.63) must vanish. Thus, the production of available potential energy by zonal-mean and eddy diabatic processes must balance the mean plus eddy kinetic energy dissipation:

$$\overline{R} + R' = -\overline{\varepsilon} - \varepsilon' \tag{10.64}$$

Because solar radiative heating is a maximum in the tropics, where the temperatures are high, it is clear that $\overline{R}$, the generation of zonal-mean potential energy by the zonal-mean heating, will be positive. For a *dry* atmosphere in which eddy diabatic processes are limited to radiation and diffusion R', the diabatic production of eddy available potential energy should be negative because the thermal radiation emitted to space from the atmosphere increases with increasing temperature and thus tends to reduce horizontal temperature contrasts in the atmosphere. For Earth's atmosphere, however, the presence of clouds and precipitation greatly alters the distribution of R'. Present estimates (Figure 10.14) suggest that in the Northern Hemisphere R' is positive and nearly half as large as $\overline{R}$. Thus, diabatic heating generates both zonal-mean and eddy available potential energy.

Equations (10.59) through (10.62) together provide a complete description of the quasi-geostrophic energy cycle from the conventional Eulerian mean

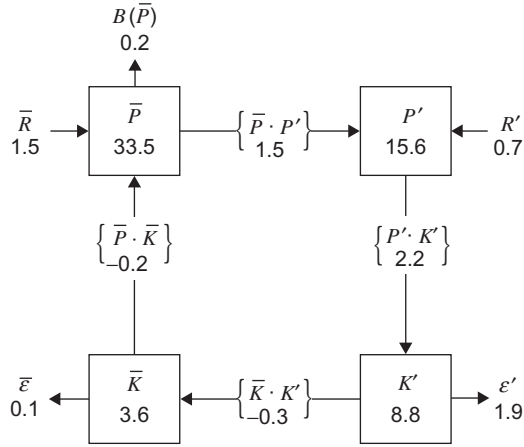

FIGURE 10.14 Observed mean energy cycle for the Northern Hemisphere. Numbers in *squares* are energy amounts in units of 10^5 J m^{-2}. Numbers *next to arrows* are energy transformation rates in units of W m^{-2}. $B(\overline{P})$ represents a net energy flux into the Southern Hemisphere. Other symbols are defined in the text. (*Adapted from Oort and Peixoto, 1974. Copyright © American Geophysical Union. Used with permission.*)

point of view. The content of these equations is summarized by means of the four-box diagram in Figure 10.14. In this diagram the squares represent reservoirs of energy, and the arrows indicate sources, sinks, and conversions. The observed direction of the conversion terms in the troposphere for the Northern Hemisphere annual mean is indicated by arrows. It should be emphasized that the direction of the various conversions cannot be theoretically deduced by reference to the energy equations alone. It also should be emphasized that the conversion terms given here are a result of the particular type of zonal average model used. The analogous energy equations for the TEM equations have rather different conversions. Thus, the energy transformations given in the present analysis should not be regarded as fundamental properties of the atmosphere but rather as properties of the Eulerian mean system.

Nevertheless, because the conventional Eulerian mean model is generally used as a basis for the study of baroclinic waves, the four-box energy diagram presented here does provide a useful framework for considering the role of weather disturbances in maintenance of the general circulation. The observed energy cycle as summarized in Figure 10.14 suggests the following qualitative picture:

1. The zonal-mean diabatic heating generates mean zonal available potential energy through a net heating of the tropics and cooling of the polar regions.
2. Baroclinic eddies transport warm air poleward and cold air equatorward, and transform the mean available potential energy to eddy available potential energy.
3. At the same time, eddy available potential energy is transformed into eddy kinetic energy by the vertical motions in the eddies.
4. The zonal kinetic energy is maintained primarily by the conversions from eddy kinetic energy due to the correlation $\overline{u'v'}$. This is discussed further in the next section.
5. The energy is dissipated by surface and internal friction in the eddies and mean flow.

In summary, the observed atmospheric energy cycle as given by the Eulerian mean formulation is consistent with the notion that baroclinically unstable eddies are the primary disturbances responsible for the energy exchange in midlatitudes. It is through the eddy motions that the kinetic energy lost through turbulent stresses is replaced, and it is the eddies that are primarily responsible for the poleward heat transport to balance the radiation deficit in the polar regions. In addition to transient baroclinic eddies, forced stationary orographic waves and free Rossby waves may also contribute substantially to the poleward heat flux. The direct conversion of mean available potential energy to mean kinetic energy by symmetric overturning is, however, small and negative in the middle latitudes but positive in the tropics, where it plays an important role in the maintenance of the mean Hadley circulation.

10.5 LONGITUDINALLY DEPENDENT TIME-AVERAGED FLOW

So far in this chapter we have concentrated on the zonally averaged component of the general circulation. For a planet with a longitudinally uniform surface, the flow averaged over a season should be completely characterized by the zonally averaged component of the circulation, since for such a hypothetical planet the statistics of zonally asymmetric transient eddies (i.e., weather disturbances) should be independent of longitude. On Earth, however, large-scale topography and continent–ocean heating contrasts provide strong forcing for longitudinally asymmetric planetary-scale time mean motions. Such motions, usually referred to as *stationary waves*, are especially strong in the Northern Hemisphere during the winter season.

Observations indicate that tropospheric stationary waves generally tend to have an equivalent barotropic structure; that is, wave amplitude generally increases with height, but phase lines tend to be vertical. Although nonlinear processes may be significant in the formation and maintenance of stationary waves, the climatological stationary wave pattern can to a first approximation be described in terms of forced barotropic Rossby waves. When superposed on zonal-mean circulation, such waves produce local regions of enhanced and diminished time mean westerly winds, which strongly influence the development and propagation of transient weather disturbances. They thus represent essential features of the climatological flow.

10.5.1 Stationary Rossby Waves

The most significant of the time mean zonally asymmetric circulation features is the pattern of stationary planetary waves excited in the Northern Hemisphere by the flow over the Himalayas and the Rockies. It was shown in Section 5.7.2 that the quasi-stationary wave pattern along 45° latitude could be accounted for to a first approximation as the forced wave response when mean westerlies impinge on the large-scale topography. More detailed analysis suggests that zonally asymmetric heat sources also contribute to the forcing of the climatological stationary wave pattern. Some controversy remains, however, concerning the relative importance of heating and orography in forcing the observed stationary wave pattern. The two processes are difficult to separate because the pattern of diabatic heating is influenced by orography.

The discussion of topographic Rossby waves in Section 5.7.2 used a β-plane channel model in which it was assumed that wave propagation was parallel to latitude circles. In reality, however, large-scale topographic features and heat sources are confined in latitude as well as longitude, and the stationary waves excited by such forcing may propagate energy meridionally as well as zonally. For a quantitatively accurate analysis of the barotropic Rossby wave response to a local source, it is necessary to use the barotropic vorticity equation in

spherical coordinates and to include the latitudinal dependence of the mean zonal wind. The mathematical analysis for such a situation is beyond the scope of this book. It is possible, however, to obtain a qualitative notion of the nature of the wave propagation for this case by generalizing the β-plane analysis of Section 5.7. Thus, rather than assuming that propagation is limited to a channel of specified width, we assume that the β plane extends to plus and minus infinity in the meridional direction and that Rossby waves can propagate both northward and southward without reflection from artificial walls.

The free barotropic Rossby wave solution then has the form of (5.109) and satisfies the dispersion relation of (5.110), where l is the meridional wave number, which is now allowed to vary. From (5.112) it is clear that for a specified zonal wave number, k, the free solution is stationary for l given by

$$l^2 = \beta/\overline{u} - k^2 \tag{10.65}$$

Thus, for example, westerly flow over an isolated mountain that primarily excites a response at a given k will produce stationary waves with both positive and negative l satisfying (10.65). As remarked in Section 5.7.1, although Rossby wave phase propagation relative to the mean wind is always westward, this is not true of the group velocity. From (5.110) we readily find that the x and y components of group velocity are

$$c_{gx} = \frac{\partial \nu}{\partial k} = \overline{u} + \beta \frac{\left(k^2 - l^2\right)}{\left(k^2 + l^2\right)^2} \tag{10.66}$$

$$c_{gy} = \frac{\partial \nu}{\partial l} = \frac{2\beta k l}{\left(k^2 + l^2\right)^2} \tag{10.67}$$

For stationary waves, these may be expressed alternatively with the aid of equation (10.65) as

$$c_{gx} = \frac{2\overline{u}k^2}{\left(k^2 + l^2\right)}, \quad c_{gy} = \frac{2\overline{u}kl}{\left(k^2 + l^2\right)} \tag{10.68}$$

The group velocity vector for stationary Rossby waves is perpendicular to the wave crests. It always has an eastward zonal component and a northward or southward meridional component depending on whether l is positive or negative. The magnitude is given by

$$\left|\mathbf{c_g}\right| = 2\overline{u}\cos\alpha \tag{10.69}$$

(see Problem 10.9). Here, as shown in Figure 10.15 for the case of positive l, α is the angle between lines of constant phase and the y axis.

Because energy propagates at the group velocity, (10.68) indicates that the stationary wave response to a localized topographic feature should consist of two wave trains, one with $l > 0$ extending eastward and northward and the other

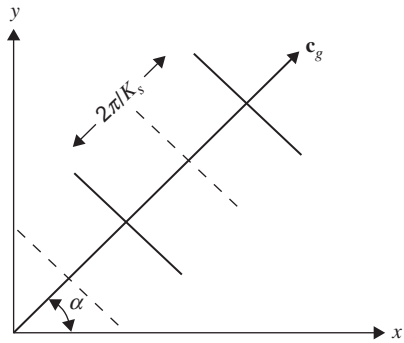

FIGURE 10.15 Stationary plane Rossby wave in a westerly flow. Ridges (*solid lines*) and troughs (*dashed lines*) are oriented at an angle α to the y axis; the group velocity relative to the ground, $\mathbf{c}_g$, is oriented at an angle α to the x axis. The wavelength is $2\,\pi/K_s$. (*Adapted from Hoskins, 1983.*)

FIGURE 10.16 Vorticity pattern generated on a sphere when a constant angular velocity westerly flow impinges on a circular forcing centered at 30°N and 45°W of the central point. Left to right, the response at 2, 4, and 6 days after the forcing is switched on. Five contour intervals correspond to the maximum vorticity response that would occur in 1 day if there were no wave propagation. *Heavy lines* correspond to zero contours. The pattern is drawn on a projection in which the sphere is viewed from infinity. (*After Hoskins, 1983.*)

with $l < 0$ extending eastward and southward. An example computed using spherical geometry is given in Figure 10.16. Although the positions of individual troughs and ridges remain fixed for stationary waves, the wave trains in this example do not decay in time, as the effects of dissipation are counteracted by energy propagation from the source at the Rossby wave group velocity.

For the climatological stationary wave distribution in the atmosphere, the excitation comes from a number of sources, both topographic and thermal, distributed around the globe. Thus, it is not easy to trace out distinct paths of wave propagation. Nevertheless, detailed calculations using spherical geometry suggest that two-dimensional barotropic Rossby wave propagation provides a reasonable first approximation for the observed departure of the extratropical time mean flow from zonal symmetry.

Rossby waves excited by isolated orographic features also play a significant role in the momentum budget. Letting the amplitude coefficient Ψ be real in

(5.109), the meridional momentum flux can be expressed as

$$\overline{u'v'} = -\overline{(\partial\psi'/\partial x)\,(\partial\psi'/\partial y)} = -\Psi^2 kl/2$$

From (10.68) it is then verified readily that if $\overline{u} > 0$,

$$c_{gy} > 0 \quad \text{implies} \quad \overline{u'v'} < 0$$
$$c_{gy} < 0 \quad \text{implies} \quad \overline{u'v'} > 0$$

Thus, westerly momentum converges into the wave source region (where the energy flux is divergent). This eddy momentum flux convergence is necessary to balance the momentum lost to the surface through the pressure torque mechanism discussed in Section 10.3.

10.5.2 Jet Stream and Storm Tracks

When the longitudinally asymmetric geopotential anomalies associated with stationary waves are added to the zonal-mean geopotential distribution, the resulting time mean field includes local regions of enhanced meridional geopotential gradient that are manifested in the wind field of the Northern Hemisphere by the Asian and North American jetstreams. The existence of these two jets can be inferred from the January mean 500-hPa geopotential height field shown in Figure 6.3. Note the strong meridional gradients in height associated with the troughs centered just east of the Asian and North American continents (the same features can be seen in annual mean charts, although with somewhat reduced intensity). The zonal flow associated with these semipermanent troughs is illustrated in Figure 6.2. In addition to the two intense jet cores in the western Pacific and western Atlantic, there is a third weaker jet centered over North Africa and the Middle East. Figure 6.2 shows dramatically the large deviations from zonal symmetry in the jet stream structure. In midlatitudes the zonal wind speed varies by nearly a factor of three between the core of the Asian jet and the area of low wind speed in western North America.

Although, as was argued earlier, the climatological stationary wave distribution on which the Asian and North American jets are superposed is apparently forced primarily by orography, the structure of the jets also appears to be influenced by continent–ocean heating contrasts. Thus, the strong vertical shear in Asian and North American jets reflects a thermal wind balance consistent with the very strong meridional temperature gradients that occur in winter near the eastern edges of the Asian and North American continents due to the contrast between warm water to the southeast and cold land to the northwest. A satisfactory description of the jet streams must account, however, not only for their thermal structure but for the westerly acceleration that air parcels must experience as they enter the jet and the deceleration as they leave the jet core.

To understand the quasi-geostrophic momentum budget in the jet streams and its relationship to the observed distribution of weather, we consider the

zonal component of the momentum equation, which (if we neglect the β effect) may be written in the form of

$$\frac{D_g u_g}{Dt} = f_0\left(v - v_g\right) \equiv f_0 v_a \tag{10.70}$$

where v_a is the meridional component of the ageostrophic wind. This equation indicates that the westerly acceleration $(Du_g/Dt) > 0)$ that air parcels experience as they enter the jet can only be provided by a poleward ageostrophic wind component $(v_a > 0)$; conversely, the easterly acceleration that air parcels experience as they leave the jet requires an equatorward ageostrophic motion. This meridional flow, together with its accompanying vertical circulation, is illustrated in Figure 10.17. Note that this secondary circulation is thermally direct upstream of the jet core. A magnitude of $v_a \sim 2-3\,\mathrm{m\,s^{-1}}$ is required

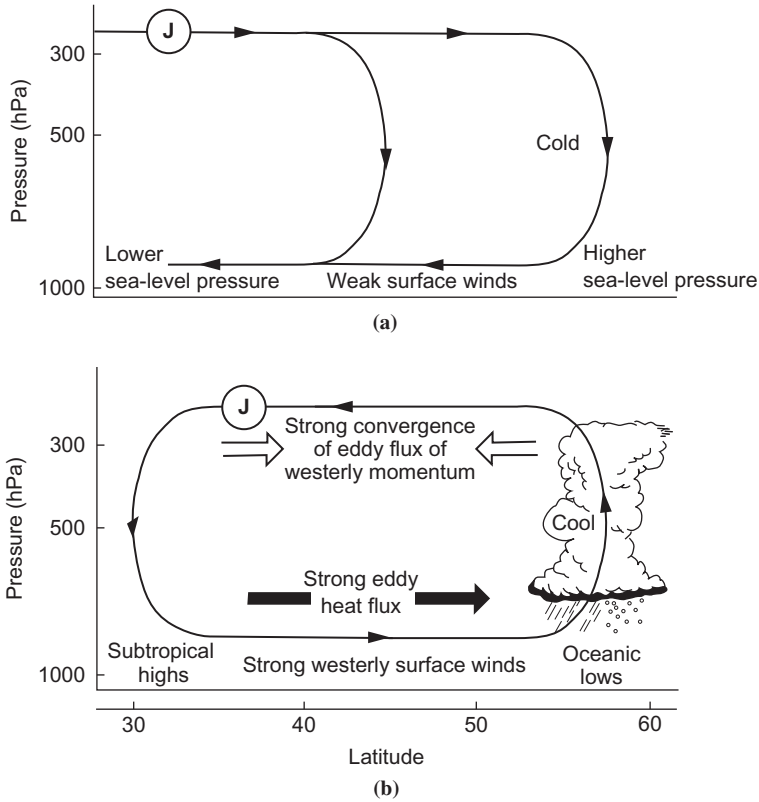

FIGURE 10.17 Meridional cross-sections showing the relationship between the time mean secondary meridional circulation (*continuous thin lines with arrows*) and the jet stream ("J") at locations (a) upstream and (b) downstream from the jet stream cores. (*After Blackmon et al., 1977. Copyright © American Meteorological Society. Reprinted with permission.*)

to account for the observed zonal wind acceleration. This is an order of magnitude stronger than the zonal-mean indirect cell (Ferrel cell) that prevails in midlatitudes. Downstream of the jet core, however, the secondary circulation is thermally indirect but much stronger than the zonally averaged Ferrel cell. It is interesting to note that the vertical motion pattern on the poleward (cyclonic shear) side of the jet is similar to that associated with deep transient baroclinic eddies in the sense that subsidence occurs to the west of the stationary trough associated with the jet, and ascent occurs east of the trough (e.g., Figure 6.18).

Because the growth rate of baroclinically unstable synoptic-scale disturbances is proportional to the strength of the basic state thermal wind, it is not surprising that the Pacific and Atlantic jet streams are important source regions for storm development. Typically, transient baroclinic waves develop in the jet entrance region, grow as they are advected downstream, and decay in the jet exit region. The role of these transient eddies in maintenance of the jet stream structure is rather complex. Transient eddy heat fluxes, which are strong and poleward in the storm tracks, appear to act to weaken the climatological jets. The transient eddy vorticity flux in the upper troposphere, however, appears to act to maintain the jet structure. In both cases the secondary ageostrophic circulation associated with the jet tends to partly balance the influence of the transient eddy fluxes in order to maintain the mean thermal and momentum balances.

10.6 LOW-FREQUENCY VARIABILITY

An understanding of the general circulation requires consideration not only of the zonal-mean and stationary wave components and their variations with the annual cycle, but also of irregular variability on time scales longer than that of individual transient eddies. The term *low-frequency variability* is generally used to describe such components of the general circulation. The observed spectrum of low-frequency variability ranges from weather anomalies lasting only 7 to 10 days to interannual variability on the scale of several years (see Section 11.1.6).

One possible cause of atmospheric low-frequency variability is forcing due to anomalies in sea surface temperature (SST), which themselves arise from coherent air–sea interaction. Because of the large thermal inertia of the oceanic surface mixed layer, such anomalies tend to have time scales much longer than those associated with subseasonal variations in the atmosphere; they are thought to be of greatest significance on the seasonal and interannual time scales.

It is believed, however, that substantial variability on subseasonal time scales can arise in midlatitudes in the absence of anomalous SST forcing as a result of internal nonlinear atmospheric dynamics, although SST anomalies may tend to favor the occurrence of certain types of variations. One example of internally generated low-frequency variability is the forcing of large-scale anomalies by potential vorticity fluxes of high-frequency transient waves. This process appears to be important in the maintenance of high-amplitude quasi-

stationary wave disturbances called *blocking* patterns. Some types of blocking may also be related to special nonlinear wave patterns called *solitary waves*, in which damping by Rossby wave dispersion is balanced by intensification due to nonlinear advection. Although most internal mechanisms involve nonlinearity, there is some evidence that the longitudinally dependent time mean flow may be unstable to linear barotropic normal modes that are stationary in space but oscillate in time at low frequencies. Such modes, which are global in scale, may be responsible for some observed teleconnection patterns.

10.6.1 Climate Regimes

It has long been observed that extratropical circulation appears to alternate between a so-called high-index state, corresponding to a circulation with strong zonal flow and weak waves, and a "low-index" state, with weak zonal flow and high-amplitude waves. This behavior suggests that more than one climate regime exists consistent with a given external forcing and that the observed climate may switch back and forth between regimes in a chaotic fashion. Whether the high-index and low-index states actually correspond to distinct quasi-stable atmospheric climate regimes is a matter of controversy.

The concept of climate regimes can also be demonstrated in a highly simplified model of the atmosphere developed by Charney and DeVore (1979). They examined the equilibrium mean states that can result when a damped topographic Rossby wave interacts with the zonal-mean flow. Their model is an extension of the topographic Rossby wave analysis given in Section 5.7.2. In this model the wave disturbance is governed by (5.118), which is the linearized form of the barotropic vorticity equation (5.113) with weak damping added. The zonal-mean flow is governed by the barotropic momentum equation:

$$\frac{\partial \overline{u}}{\partial t} = -D(\overline{u}) - \kappa(\overline{u} - U_e) \tag{10.71}$$

where the first term on the right designates forcing by interaction between the waves and the mean flow, and the second term represents a linear relaxation toward an externally determined basic state flow, U_e.

The zonal mean equation (10.71) can be obtained from (5.113) by dividing the flow into zonal-mean and eddy parts and taking the zonal average to get

$$\frac{\partial}{\partial t}\left(-\frac{\partial \overline{u}}{\partial y}\right) = -\frac{\partial}{\partial y}\left(\overline{v_g' \zeta_g'}\right) - \frac{f_0}{H}\frac{\partial}{\partial y}\left(\overline{v_g' h_T}\right)$$

which, after integrating in y and adding the external forcing term, yields (10.71) with

$$D(\overline{u}) = -\overline{v_g' \zeta_g'} - \left(f_0 / H\right)\overline{v_g' h_T} \tag{10.72}$$

As shown in Problem 10.5, the eddy vorticity flux, that is, the first term on the right in (10.72), is proportional to the divergence of the eddy momentum

flux. The second term, which is sometimes referred to as the *form drag*, is the equivalent in the barotropic model of the surface pressure torque term in the angular momentum balance equation (10.43).

If h_T and the eddy geostrophic streamfunction are assumed to consist of single harmonic wave components in x and y, as given by (5.115) and (5.116), respectively, the vorticity flux vanishes, and with the aid of (5.119) the form drag can be expressed as

$$D(\bar{u}) = -\left(\frac{f_0}{H}\right)\overline{v_g' h_T} = \left(\frac{rK^2 f_0^2}{2\bar{u}H^2}\right)\frac{h_0^2 \cos^2 ly}{\left[\left(K^2 - K_s^2\right)^2 + \varepsilon^2\right]} \tag{10.73}$$

where r is the spin-down rate due to boundary layer dissipation, ε is as defined in equation (5.119), and K_s is the resonant stationary Rossby wave number defined in (5.112).

It is clear from (10.73) that the form drag will have a strong maximum when $\bar{u} = \beta/K^2$, as shown schematically in Figure 10.18. The last term on the right in (10.71), however, will decrease linearly as $\bar{u}$ increases. Thus, for suitable parameters there will be three values of $\bar{u}$ (labeled A, B, and C in Figure 10.18) for which the wave drag just balances the external forcing so that steady-state solutions may exist. By perturbing the solution about the points A, B, and C, it is shown easily (Problem 10.12) that point B corresponds to an unstable equilibrium, whereas the equilibria at points A and C are stable. Solution A corresponds

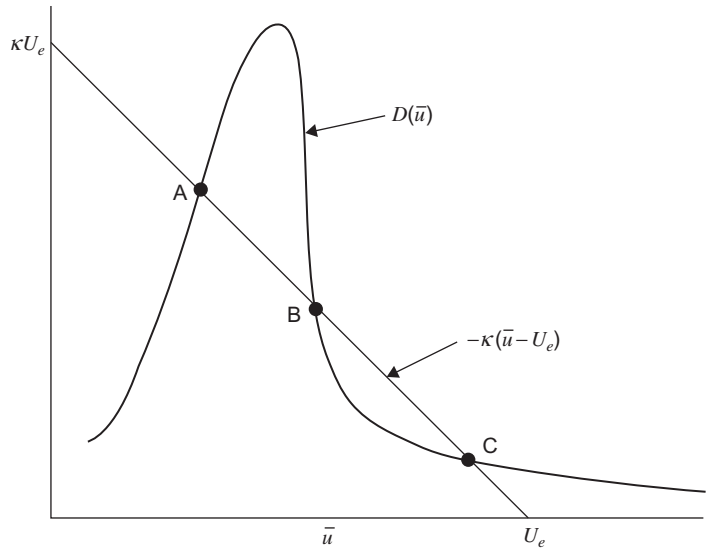

FIGURE 10.18 Schematic graphical solution for steady-state solutions of the Charney–DeVore model. (*Adapted from Held, 1983.*)

to a low-index equilibrium, with high-amplitude waves analogous to a blocking regime. Solution C corresponds to a high-index equilibrium with strong zonal flow and weak waves. Thus, for this very simple model there are two possible "climates" associated with the same forcing.

The Charney–DeVore model is a highly oversimplified model of the atmosphere. Models that contain more degrees of freedom do not generally have multiple steady solutions. Rather, there is a tendency for the (unsteady) solutions to cluster about certain climate regimes and to shift between regimes in an unpredictable fashion. Such behavior is characteristic of a wide range of nonlinear dynamical systems and is popularly known as *chaos* (see Section 13.7).

10.6.2 Annular Modes

If a second meridional mode is added to the Charney–DeVore model (see Exercise M10.2), oscillatory solutions can be obtained that bear a qualitative resemblance to the observed leading modes of variability in the extratropical atmospheric circulation in both hemispheres. These observed modes, referred to as *annular modes*, are characterized by geopotential anomalies of opposite signs in the polar and midlatitude regions and by corresponding mean zonal wind anomalies with opposite signs equatorward and poleward of about 45° latitude (Figure 10.19). The annular modes exist year-round in the troposphere, but are strongest in the winter when they extend well into the stratosphere, especially in the Northern Hemisphere. The zonally symmetric mean flow anomalies associated with the annular modes are apparently maintained by anomalous eddy momentum fluxes, which are themselves influenced by the zonally symmetric flow anomalies.

There is some evidence for downward propagation of the wintertime annular modes, suggesting that circulation changes in the stratosphere may precede annular mode changes in the troposphere. Dynamical linkages between the stratosphere and the troposphere are discussed further in Chapter 12.

10.6.3 Sea Surface Temperature Anomalies

Sea surface temperature anomalies influence the atmosphere by altering the flux of latent and sensible heat from the ocean, and thus providing anomalous heating patterns. The efficacy of such anomalies in exciting global-scale responses depends on their ability to generate Rossby waves. A thermal anomaly can generate a Rossby wave response only by perturbing the vorticity field. This requires that the thermal anomaly produce an anomalous vertical motion field, which in turn produces anomalous vortex tube stretching.

For low-frequency disturbances the thermodynamic energy equation (10.5) may be approximated as

$$\mathbf{V} \cdot \nabla T + wN^2 HR^{-1} \approx J/c_p \tag{10.74}$$

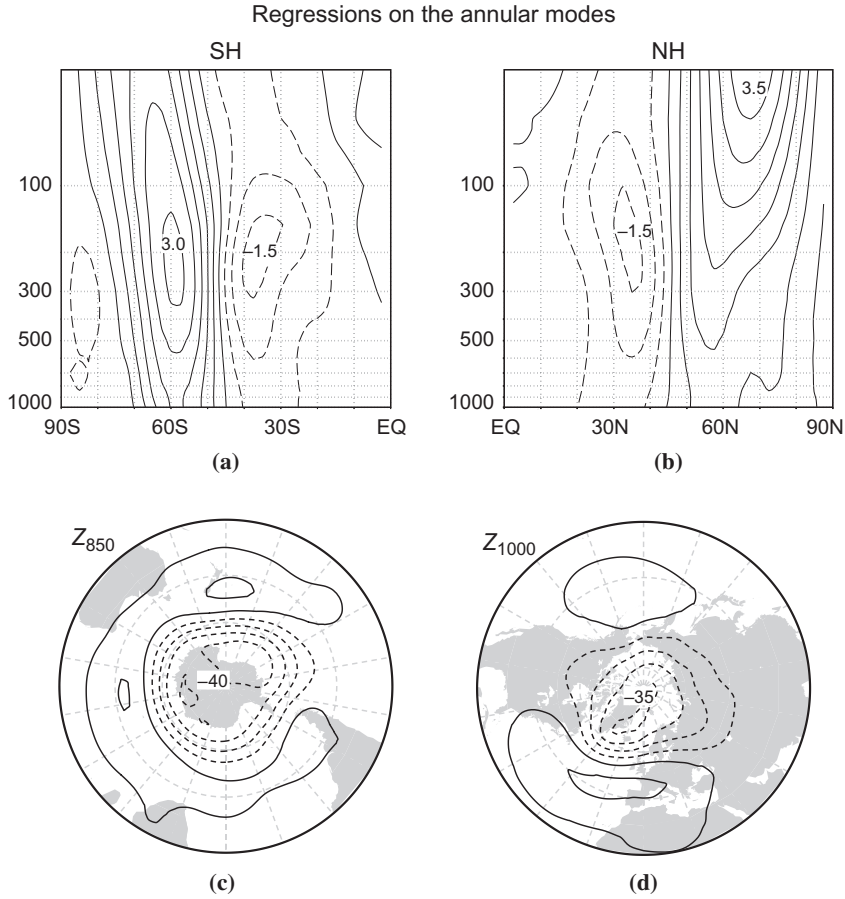

FIGURE 10.19 (a,b) Latitude–height cross-sections showing typical amplitudes of annular mode anomalies for mean-zonal wind (ordinate labels are pressure in hPa, contour interval 0.5 m s^{-1}). (c,d) Lower tropospheric geopotential height (contour interval 10 m). The Southern Hemisphere (SH) is on the *left* and the Northern Hemisphere (NH) is on the *right*. Phase shown corresponds to the high-index state (strong polar vortices). The low-index state would have opposite signed anomalies. (*After Thompson and Wallace, 2000. Copyright © American Meteorological Society. Reprinted with permission.*)

Thus, diabatic heating can be balanced by horizontal temperature advection or by adiabatic cooling due to vertical motion. The ability of diabatic heating produced by a sea surface temperature anomaly to generate Rossby waves depends on which of these processes dominates. In the extratropics, SST anomalies primarily generate low-level heating, which is balanced mainly by horizontal temperature advection. In the tropics, positive SST anomalies are associated with enhanced convection, and the resulting diabatic heating is balanced by adiabatic cooling. Tropical anomalies have their greatest effect in the

Western Pacific, where the average sea surface temperature is very high so that even a small positive anomaly can generate large increases in evaporation due to the exponential increase of saturation vapor pressure with temperature. By continuity of mass, the upward motion in cumulonimbus convection requires convergence at low levels and divergence in the upper troposphere.

The low-level convergence acts to sustain the convection by moistening and destabilizing the environment, whereas the upper-level divergence generates a vorticity anomaly. If the mean flow is westerly in the region of upper-level divergence, the forced vorticity anomaly will form a stationary Rossby wave train. The observed upper tropospheric height anomalies during the Northern Hemisphere winter associated with such an anomaly are shown schematically in Figure 10.20. The pattern strongly suggests a train of stationary Rossby waves that emanates from the equatorial source region and follows a great circle path, as predicted by barotropic Rossby wave theory (see Section 10.5.1). In this manner, tropical SST anomalies may generate low-frequency variability in the extratropics. It is possible that the effects of SST anomalies and of internal variability are not completely independent. In particular, it is more likely that the atmosphere will tend to preferentially reside in those regimes whose anomalous flow is correlated with the pattern in Figure 10.20 than would be the case in the absence of SST anomalies.

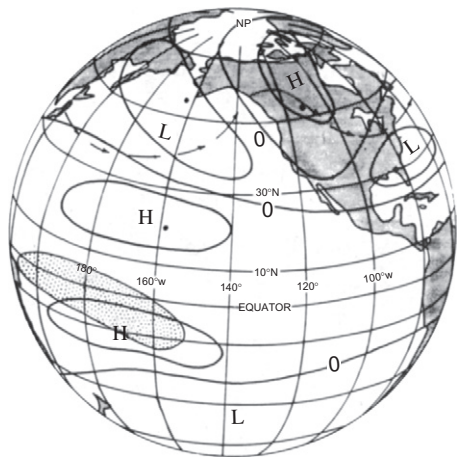

FIGURE 10.20 Pattern of middle and upper tropospheric height anomalies for Northern Hemisphere winter during an ENSO event in the tropical Pacific. The region of enhanced tropical precipitation is shown by *shading*. *Arrows* depict a 200-hPa streamline for the anomaly conditions. "H" and "L" designate anomaly highs and lows, respectively. The anomaly pattern propagates along a great circle path with an eastward component of group velocity, as predicted by stationary Rossby wave theory. (*After Horel and Wallace, 1981. Copyright © American Meteorological Society. Reprinted with permission.*)

10.7 NUMERICAL SIMULATION OF THE GENERAL CIRCULATION

The only practical manner in which to quantitatively simulate the present climate, or to predict possible climate modifications resulting from intentional or unintentional human intervention, is by numerical simulation with the aid of computers. Atmospheric general circulation models (AGCMs) are similar to large-scale numerical weather prediction models (see Chapter 13) in that they attempt to explicitly simulate synoptic-scale weather disturbances. However, whereas weather prediction is an *initial value* problem, which requires that the evolution of the flow be computed from a specified initial state, general circulation modeling is usually performed as a *boundary value* problem in which the average circulation is computed for specified external forcing conditions.

In many AGCMs the sea surface temperature is treated as a specified forcing. In reality, of course, there are strong interactions between the atmosphere and the ocean: The winds drive currents, which influence the sea surface temperature distribution, which in turn influences the atmosphere. Such interaction may be simulated using *coupled climate models*, also known as Earth system models (ESMs), which include flux couplers that link the atmosphere with other constituent components of the climate system, including the ocean, land surface, biosphere, and cryosphere. Unlike the dynamical cores of AGCMs, which involve numerical solution of the equations of dynamic meteorology and may be compared against known analytical nonlinear solutions on the sphere, there are no known solutions of the full coupled system. Therefore, for ESMs, validation typically comprises a comparison of simulated statistics with observations during the instrumental record.

Atmospheric model intercomparison projects (AMIPs) provide a standardized experimental design that is meant to facilitate comparing the performance of different models by fixing many aspects of the simulation. Experiments are configured with prescribed sea surface temperature and sea–ice boundary conditions, along with the concentration and distribution of radiatively important gases such as ozone and carbon dioxide. Similarly, the coupled model intercomparison project (CMIP) provides a standardized protocol for comparing ESMs. The collected datasets for AMIPs and CMIPs provide a large sample of information that has proven useful for climate studies and model comparisons; data from these experiments are freely available on the Web.

Interest in the development of AGCMs and ESMs derives not only from the pursuit of basic research but also from societal interest in predicting future climate. Periodic reports from the Intergovernmental Panel on Climate Change (IPCC) provide a comprehensive summary of the results from these model projections, and also a thorough review of the latest results in climate research. Forecasts described in these reports have been consistent in projecting, relative to preindustrial times, about 2.0 to 4.5°C warming of the global-mean surface

temperature due to a presumed doubling of carbon dioxide. Projections also show a small, but nontrivial, probability that the warming may be much larger. An introduction to climate sensitivity analysis in Section 10.8 will serve to provide a quantitative basis for understanding the source of this disturbingly wide range of uncertainty.

Because of its enormous complexity and many important applications, general circulation modeling has become a complicated activity that cannot possibly be covered adequately in a short space. Here we can only give a summary of the primary physical processes represented and present an example of an application in climate modeling. A brief discussion of the technical aspects of the formulation of numerical prediction models is given in Chapter 13.

10.7.1 Dynamical Formulation

Most general circulation models are based on the primitive equations in the σ-coordinate form introduced in Section 10.3.1. As was pointed out in that section, σ coordinates make it possible to retain the dynamical advantages of pressure coordinates but simplify the specification of boundary conditions at the surface.

The minimum prediction equations for a σ-coordinate GCM are the horizontal momentum equation (10.30), the mass continuity equation (10.34), the thermodynamic energy equation (10.36), and a moisture continuity equation, which can be expressed as

$$\frac{D}{Dt}(q_v) = P_v \tag{10.75}$$

where q_v is the water vapor mixing ratio and P_v is the sum of all sources and sinks. In addition, we require the hydrostatic equation (10.35) to provide a diagnostic relationship between the geopotential and temperature fields. Finally, a relationship is needed to determine the evolution of the surface pressure $p_s(x, y, t)$. This is given by integrating (10.34) vertically and using the boundary conditions $\dot{\sigma} = 0$ at $\sigma = 0$ and 1 to obtain

$$\frac{\partial p_s}{\partial t} = -\int_0^1 \nabla \cdot (p_s \mathbf{V}) d\sigma \tag{10.76}$$

Vertical variations are generally represented by dividing the atmosphere into a number of levels and utilizing a finite difference grid. AGCMs typically have prediction levels at 1- to 3-km intervals extending from the surface to about a 30-km altitude. Some models, however, have many more levels extending nearly to the mesopause. Horizontal resolution of global models varies widely, from an effective grid size of several hundred kilometers to less than 100 km.

10.7.2 Physical Processes and Parameterizations

The various types of surface and atmospheric processes represented in a typical AGCM and the interactions among these processes are shown schematically in Figure 10.21. The most important classes of physical processes are (1) radiative, (2) cloud and precipitation, and (3) turbulent mixing and exchange.

As pointed out in Section 10.1, the fundamental process that drives the circulation of the atmosphere is the differential radiative heating that results in a net gain in heat at low latitudes relative to high latitudes. The general circulation of

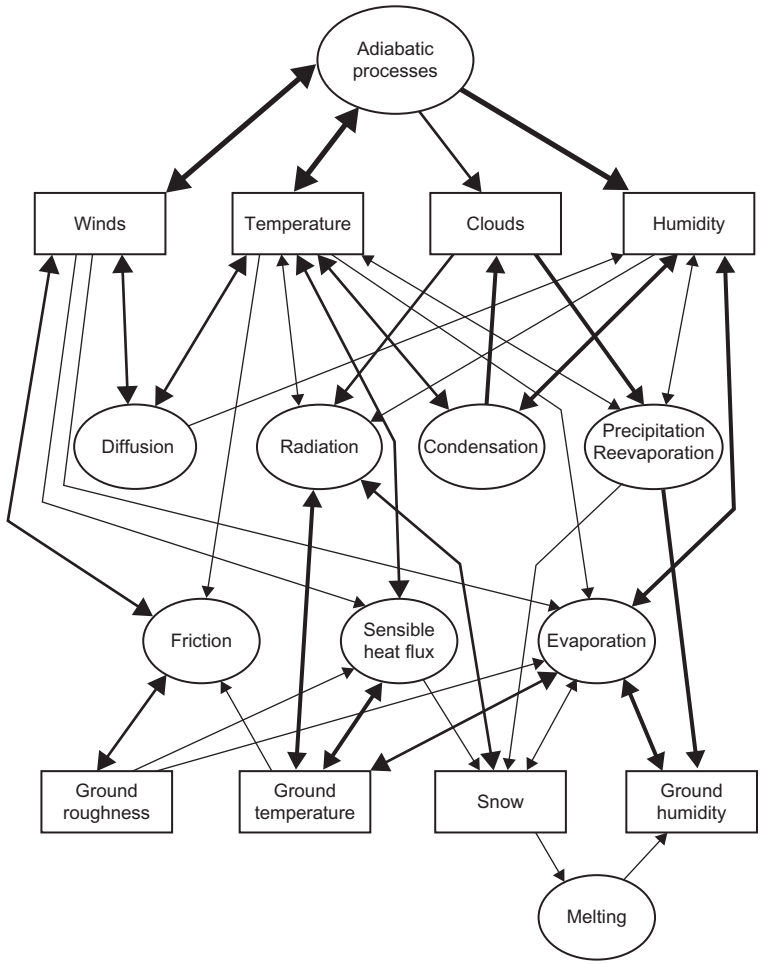

FIGURE 10.21 Schematic of processes commonly included in AGCMs and their interactions. The *thickness* of each arrow gives a rough indication of the importance of the interaction that a particular arrow represents. (*After Simmons and Bengtsson, 1984. Copyright © Cambridge University Press. Used with permission.*)

the atmosphere and the oceans provides the meridional and vertical heat transfer required for balance.

Half of the solar radiation absorbed at the surface is used to evaporate water and thus to moisten the atmosphere. Solar heating is realized in the atmosphere primarily in the form of latent heat release associated with convective clouds. The global distribution of evaporation clearly depends on the sea surface temperature, which is itself dependent on the general circulation of the oceans as well as on interactions with the atmosphere. That is why, for detailed understanding of the influence of large-scale air–sea interactions on climate, it is important to run coupled atmosphere–ocean GCMs in which the sea surface temperature is predicted. At present, however, most AGCMs use externally specified monthly or seasonal mean sea surface temperatures. Over land, however, the surface temperature adjusts very quickly to changes in the fluxes of solar and infrared radiation and is determined from a surface energy–balance equation.

Atmospheric radiative heating by solar radiation and heating and cooling by long-wave thermal radiation are computed using radiative transfer models of varying sophistication. Zonally averaged distributions of radiatively important constituents such as carbon dioxide, ozone, and even cloudiness are often employed, but the more complete models do utilize model-predicted zonally and time-varying cloudiness in their radiation codes.

Boundary layer fluxes of momentum, heat, and moisture are parameterized in most AGCMs by the use of bulk aerodynamic formulas (see Section 8.3.1). Typically the fluxes are specified to be proportional to the magnitude of the horizontal velocity at the lowest atmospheric level times the difference between the field variable at the boundary and its value at the lowest atmospheric level. In some models the boundary layer is explicitly resolved by locating several prediction levels within the lowest 2 km and utilizing the model-predicted boundary layer static stability in the parameterization of turbulent fluxes.

The hydrological cycle is usually represented by a combination of parameterization and explicit prediction. The water vapor mixing ratio is generally one of the explicitly predicted fields. The distributions of layer clouds and large-scale precipitation are then determined from the predicted distribution of humidity by requiring that when the predicted humidity exceeds 100%, enough vapor is condensed to reduce the mixing ratio to saturation or less. Parameterizations in terms of the mean state thermal and humidity structure must be used to represent the distributions of convective clouds and precipitation.

10.8 CLIMATE SENSITIVITY, FEEDBACKS, AND UNCERTAINTY

As discussed previously, ESMs predict warming of about 3°C under a scenario of doubling carbon dioxide concentration over preindustrial values, but the probability distribution of forecasts is skewed, with a long tale extending toward much larger warming. To understand the source of this uncertainty, we briefly

review climate sensitivity analysis, which is typically defined as the change in the global-mean temperature, from one equilibrium state to another, due to an imposed forcing that changes the heat budget of the Earth system. Assuming that the change is small, we may estimate it by the leading-order Taylor series approximation

$$T(R_0 + \delta R) \;=\; T(R_0) + \left.\frac{\partial T}{\partial R}\right|_{R_0} \delta R \tag{10.77}$$

Here, the global-mean surface temperature, T, in equilibrium, is assumed to depend only on the parameter R, which may be taken as the net radiative heating of the surface, and R_0 is the value for the unperturbed climate. The linear response to perturbing the radiative heating by δR is then given by

$$\delta T \;=\; \left.\frac{\partial T}{\partial R}\right|_{R_0} \delta R \;=\; \lambda\, \delta R \tag{10.78}$$

where λ is the climate sensitivity parameter, which determines the change in temperature for a given amount of forcing. A common experiment with climate models used to determine λ involves perturbing the carbon dioxide field by instantaneously doubling the concentration and then integrating the model to a new equilibrium state (when the global-mean surface temperature reaches a new time-averaged value). Results show an initial, relatively fast, response due to strong greenhouse forcing, with about half of the warming occurring in about 50 years, followed by a slower asymptotic approach to the new equilibrium value, which may take over 1000 years.

The evolution to a new equilibrium state involves an interaction between various aspects of the Earth system, including feedback processes, which will be discussed next. In the absence of feedbacks, the experiments described previously produce a warming of about $\delta T_0 = 1.2^{\circ}\mathrm{C}$ due to δR_0 of roughly 4 W m^{-2}, yielding a "control" climate sensitivity of 0.3 K(W m^{-2})$^{-1}$. Feedbacks may increase or decrease this control value by an amount proportional to the "output," δT:

$$\delta T = \delta T_0 + f \delta T \tag{10.79}$$

where "feedback factor" f controls the amplification. Feedbacks are due to physical processes that depend on temperature, such as clouds, which affect the radiative forcing. Therefore, we take $R(\alpha_i(T))$, where α_i represents the physical process, so that application of the chain rule in (10.78) gives

$$\delta T \;=\; \lambda\, \delta R_0 + \lambda \sum_i \frac{\partial R}{\partial \alpha_i} \frac{\partial \alpha_i}{\partial T} \delta T \tag{10.80}$$

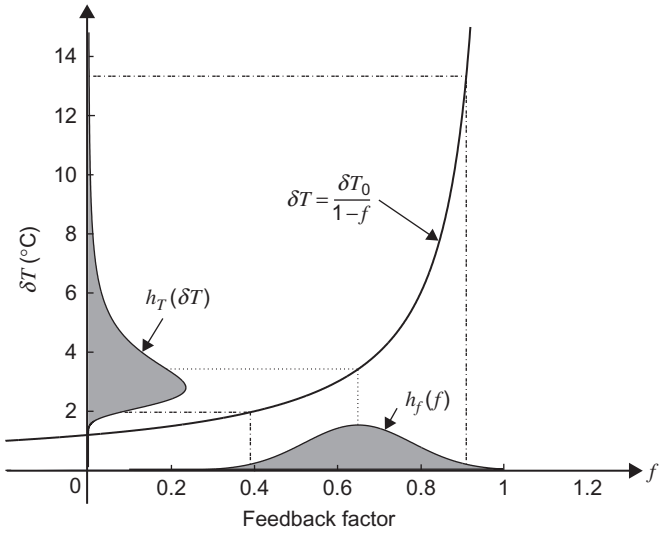

FIGURE 10.22 How (10.82) (*solid curve*) maps uncertainty in the feedback factor, f (abscissa) onto uncertainty in the temperature equilibrium change, δT (ordinate). *Gray shading* gives the probability density function, with a Gaussian distribution assumed for the feedback factor for purpose of illustration. The control equilibrium temperature change is taken to be 3°C. *Dotted* (*dashed*) *lines* show the mean (95% confidence interval) for the feedback factor. (*Adapted with permission from Roe and Baker, 2007.*)

This result is the same as (10.79) provided that the feedback factor is defined by

$$f = \lambda \sum_i \frac{\partial R}{\partial \alpha_i} \frac{\partial \alpha_i}{\partial T} \tag{10.81}$$

Solving (10.79) for δT gives

$$\delta T = \frac{\delta T_0}{1 - f} \tag{10.82}$$

If the feedback parameter is positive, the feedbacks amplify the control response to a given forcing; $f \geq 1$ represents unphysical solutions. Note that since $1/(1-f)$ is a nonlinear function,[3] small changes in f may lead to large changes in δT. This fact is graphically depicted in Figure 10.22 and reveals the essence of the uncertainty in climate forecasts. Climate models approximate the natural system, with many sources of uncertainty, which implies uncertainty in the feedback factor (assumed Gaussian in Figure 10.22). This feedback uncertainty

[3]In the limit of the small feedback factor, $1/(1-f) \approx 1 + f$. This is linear feedback, which is consistent with (10.79) when the feedback is proportional to the control value, $\delta T = \delta T_0 + f\delta T_0$, and with (10.80) when the processes, α_i, do not depend on temperature.

maps into a non-Gaussian distribution in δT with a "long tail" of large warming (8–12°C) relative to the peak of the distribution (3°C). Reducing the long tail requires narrowing the distribution for the feedback factor. Since the total feedback factor is a sum of many feedback processes (see 10.80), this presents a daunting task in complex Earth System models, but may be more tractable in simpler models that are properly calibrated.

Of the many feedbacks in ESMs, the following are currently thought to be the most important:

1. The **water vapor feedback** results from the fact that, through the Clausius-Clapeyron equation, the saturation vapor pressure of water vapor increase with temperature. Water vapor is the most important greenhouse gas in Earth's atmosphere, so unless the relative humidity changes, a positive feedback results when the temperature increases because of, for example, CO_2 forcing, since the amount of water vapor in the atmosphere increases, producing more warming. Conversely, forcing that produces cooling reduces the saturation vapor pressure, leading to more cooling.
2. The **ice–albedo feedback** is due to the fact that ice strongly reflects solar radiation so that decreasing the amount of ice reduces the planetary albedo, thereby increasing the temperature and producing more ice loss. Conversely, increasing the amount of ice increases the planetary albedo, thereby decreasing the temperature, which further increases the amount of ice.
3. **Cloud feedback** comes in a wide variety, but one particularly simple one involves the areal coverage of low clouds. Low clouds emit radiation near the surface temperature, so they have little effect on outgoing long-wave radiation, but since they are highly reflective, they can reduce the net incoming solar radiation. Therefore, if warming results in substantially less low cloud, a positive feedback occurs since the planetary albedo decreases, producing more warming. Conversely, if warming results in more low cloud, a negative feedback results.
4. The **lapse-rate feedback** derives from the fact that, especially in the tropics, the lapse rate tends to follow a saturated adiabat. Since saturated adiabats become less steep with increasing temperature (more latent heat is available to offset adiabatic cooling for lifted parcels), a negative feedback results because smaller lapse rates result in less warming. Conversely, decreasing the temperature increases the lapse rate, resulting in more cooling.

SUGGESTED REFERENCES

James, *Introduction to Circulating Atmospheres*, provides an excellent introduction to observational and theoretical aspects of the global general circulation.

Lorenz, *The Nature and Theory of the General Circulation of the Atmosphere*, although somewhat out of date, contains an excellent survey of the subject, including observational and theoretical aspects.

Randall (ed.), *General Circulation Model Development*, contains articles describing all aspects of general circulation modeling.

Schneider (2006) provides a modern review of the general circulation.

Washington and Parkinson, *An Introduction to Three-Dimensional Climate Modeling*, provide an excellent text, which covers the physical basis and computational aspects of general circulation modeling.

PROBLEMS

10.1. Starting with the isobaric version of the thermodynamic energy equation (2.42), derive the log-pressure version (10.5).

10.2. Show that in the σ-coordinate system a mass element $\rho_0 dxdydz$ takes the form $-g^{-1}p_s dxdyd\sigma$.

10.3. Compute the mean zonal wind $\bar{u}$ at the 200-hPa level at 30°N under the assumption that $\bar{u} = 0$ at the equator and that the absolute angular momentum is independent of latitude. What is the implication of this result for the role of eddy motions?

10.4. Show by scale analysis that advection by the mean meridional circulation can be neglected in the zonally averaged equations (10.11) and (10.12) for quasi-geostrophic motions.

10.5. Show that for quasi-geostrophic eddies the next to last term in square brackets on the right side in (10.15) is proportional to the vertical derivative of the eddy meridional relative vorticity flux.

10.6. From equations (10.16) through (10.19), derive the governing equation for the residual streamfunction (10.21).

10.7. Using the observed data given in Figure 10.13, compute the time required for each possible energy transformation or loss to restore or deplete the observed energy stores. (A watt equals 1 $\mathrm{J\,s^{-1}}$.)

10.8. Compute the surface torque per unit horizontal area exerted on the atmosphere by topography for the following distribution of surface pressure and surface height:

$$p_s = p_0 + \hat{p}\sin kx, \quad h = \hat{h}\sin(kx - \gamma)$$

where $p_0 = 1000$ hPa, $\hat{p} = 10$ hPa, $\hat{h} = 2.5 \times 10^3$ m, $\gamma = \pi/6$ rad, and $k = 1/(a\cos\phi)$, where $\phi = \pi/4$ radians is the latitude, and a is Earth's radius. Express the answer in $\mathrm{kg\,s^{-2}}$.

10.9. Starting from (10.66) and (10.67), show that the group velocity relative to the ground for stationary Rossby waves is perpendicular to the wave crests and has a magnitude given by (10.69).

10.10. Consider a thermally stratified liquid contained in a rotating annulus of inner radius 0.8 m, outer radius 1.0 m, and depth 0.1 m. The temperature at the bottom boundary is held constant at T_0. The fluid is assumed to satisfy the equation of state (10.76) with $\rho_0 = 10^3$ $\mathrm{kg\,m^{-3}}$ and $\varepsilon = 2 \times 10^{-4}$ $\mathrm{K^{-1}}$. If the temperature increases linearly with height along the outer radial boundary at a rate of 1°C $\mathrm{cm^{-1}}$ and is constant with height along the inner radial boundary, determine the geostrophic velocity at the upper boundary for a rotation rate of $\Omega = 1$ rad $\mathrm{s^{-1}}$. (Assume that the temperature depends linearly on radius at each level.)

10.11. Show by considering $\partial\overline{u}/\partial t$ for small perturbations about the equilibrium points in Figure 10.18 that point B is an unstable equilibrium point while points A and C are stable.

MATLAB Exercises

M10.1. The MATLAB script **topo_wave_1.m** uses finite differencing to solve the linearized vorticity equation (5.118) on a midlatitude β plane for the case of a constant mean zonal wind and forcing by a circular mountain with mountain height given by $h_T(x, y) = h_0 L^2 \left(L^2 + x^2 + y^2\right)^{-1}$, where h_0 and L are constants characterizing the mountain height and horizontal scale, respectively. Run the script for mean zonal winds of 5, 10, 15, and 20 $\mathrm{m\,s^{-1}}$. In each case estimate the horizontal wavelength and group velocity of the northward and southward Rossby wave trains that form in the lee of the mountain. Compare your results with the corresponding expressions given in Section 10.5.1.

M10.2. The two-meridional-mode version of the Charney and Devore (1979) model described in Section 10.6.1 is given in the MATLAB script **C_D_model.m**. Solutions for this model may be steady state, periodic in time, or irregularly varying, depending on the forcing of the first mode zonal-mean streamfunction (`zf(1)` in the script) and the initial amplitude of this mode (`zinit(1)` in the script). Run this script for forcing values of `zf(1) = 0.1, 0.2, 0.3, 0.4, 0.5`. In each case do two runs with initial conditions `zinit(1) = zf(1)` and `zinit(1) = 0.1`, respectively. For each of the 10 cases, note whether the solution is steady, periodic, or irregular. Compute the time average of the zonal mean zonal wind for nondimensional time interval $2000 < t < 3000$ for each of these cases. Are your results consistent with Figure 10.18? Note for each case whether the streamfunction tends to be in phase or out of phase with the topography and whether the results are qualitatively consistent with the solution for topographic Rossby waves given in Section 5.7.2.

M10.3. The MATLAB script **baroclinic_model_1.m** provides a simple illustration of the effect of baroclinic eddies on the mean flow. The script extends the two-level baroclinic instability model discussed in Section 7.2 by calculating the evolution of the mean zonal flow components U_m and U_T caused by meridional vorticity and heat fluxes associated with unstable baroclinic waves. The calculation is done for a midlatitude β plane with weak Ekman layer damping. The eddies are governed by the linearized model of Section 7.2 (with fixed zonal wavelength of 6000 km), but the zonal-mean flow is affected by eddy–mean flow interactions and evolves as a result of eddy heat and momentum fluxes. In this model the mean thermal wind is relaxed toward a baroclinically unstable radiative equilibrium state (designated by `U0rad` in the code), which has a sinusoidal distribution in the meridional direction, and the mean wind components U_m and U_T are assumed to vanish at the northern and southern boundaries. Run the model for four cases with `U0rad = 10, 20, 30, and 40` $\mathrm{m\,s^{-1}}$, respectively. In each case run the model long enough so that the eddy kinetic energy equilibrates. Show in a table the maximum values for U_m and U_T for each of these cases. Explain these results in terms of the baroclinic instability theory of Section 7.2.